Novel Combination Therapy: Monensin Potentiates Erlotinib-Induced Cytotoxicity.

Khalil Dayekh

Thesis submitted to the

Faculty of Graduate and Postdoctoral Studies

In partial fulfillment of the requirements

for the degree of Master's of Science in Biochemistry

Specializing in Human and Molecular Genetics

Department of Biochemistry, Microbiology, and Immunology

Faculty of Medicine

University of Ottawa

Abstract:

Receptor Tyrosine Kinase (RTK) inhibitors, such as erlotinib/tarceva, have been introduced in the past decade as a promising therapeutic option in Head and Neck Squamous Cell Carcinoma (HNSCC), however, they lack significant efficacy as single agents. As a result, RTK inhibitors require a combination based therapeutic approach with other treatment modalities. To uncover such a combination of agents, we performed a high throughput Prestwick library screen that included 1200 compounds approved by the FDA on HNSCC cell lines and found that monensin, a coccidial antibiotic, synergistically enhanced the cytotoxicity of erlotinib. RT-PCR revealed that monensin induced the expression of Activation of Transcription Factor (ATF) 3 and its downstream target C/EBP homologous protein (CHOP) which are key regulators of apoptosis. Furthermore, RNA-Seq analysis suggests that monensin augments erlotinib cytotoxicity by disturbing lipid and sterol biosynthesis. Therefore, identifying the mechanism of action exerted by monensin may open alternative avenues of cancer treatment.

Acknowledgments

First, I would like to thank my supervisor Dr. Jim Dimitroulakos for his continued assistance and support throughout the period of my studies as a Master's student and for always pointing me in the right direction when I needed guidance. Next, I would like to thank Ivan Gorn-Hundrmann, our lab technician who helped me a lot during my work in the lab. I also like to thank my colleagues who made my experience in the lab enjoyable and educating. And lastly, a big thank you goes to my family and friends who have always supported and encouraged me and kept my morale high all the way through this demanding period of my life.

Table of Contents

List of Abbreviations

AKT	Protein kinase B
ADP	Adenosine Diphosphate
ATCC	American Type Culture Collection
ATF3	Activating transcription Factor 3
ATF4	Activation of Trascription Factor 4
ATP	Adenosine Triphosphate
BCA	BiCinchoninic Acid
BNIP3	BCL2/Adenovirus E1B 19 kDa Protein-Interacting Protein 3
BSA	Bovine Serum Albumin
CDK	Cyclin Dependent Kinase
CHOP	C/EBP homologous protein
DAPK	Death-Associated Protein Kinase
DDIT3	DNA Damage-Inducible Transcript 3
DDIT4	DNA-damage-inducible transcript 4 protein
DMEM	Dulbecco's Modified Eagle's Medium
DTT	1,4-dithio-DL-threitol
EDTA	EthyleneDiamineTetraacetic Acid
EGF	Epidermal Growth Factor
EGFR	Epidermal Growth Factor Receptor
ERK	Extracellular signal Regulated Kinase
FDA	Food and Drug Administration
FPP	Farnesyl Pyrophosphate
GAPDH	GlycerAldehyde 3-Phosphate Dehydrogenase
GDP	Guanosine Diphosphate
GGPP	Geranylgeranyl Pyrophosphate
GPCR	G-Protein Coupled Receptor
GRB	Growth Factor Receptor Binding Protein
GTP	Guanosine Triphosphate
HB-EGF	Heparin-Binding EGF-like Growth Factor
HMG-CoA	Hydroxy 3-methylglutaryl-coenzyme A
HMGCR	HMG-CoA Reductase
HMGCS1	HMG-CoA Synthase 1
HNSCC	Head and Neck Squamous Cell Carcinoma
HPV	Human Papilloma Virus
HRP	Horseradish peroxidase
IGFR	Insulin Growth Factor Receptor
IgG	Immunoglobulin G
INSIG1	Insulin Induced Gene 1
ISR	Integrated Stress Response
JAK	Janus Kinase
LDL	Low Density Lipoproteins
MAbs	Monoclonal Antibodies

MAPK	Mitogen Activated Protein Kinase
MEK	Mitogen activated protein kinase kinase
MTT	3-(4,5-Dimethylthiazol-2-yl)- 2,5-Diphenyltetrazolium bromide
NSCLC	Non-Small Cell Lung Carcinoma
OHRI	Ottawa Hospital Research Institute
PARP	Poly ADP-Ribose Polymerase
PBS	Phosphate buffered saline
PCSK9	Proprotein convertase subtilisin/kexin type 9
PI3K	Phosphatidylinositide 3 Kinase
PLC	Phospholipase C
Ras	Rat sarcoma
RHOA	Ras Homolog A
RIPA	Radio Immuno-Pricipitation Assay
RISC	RNA-Induced Silencing Complex
RTK	Receptor Tyrosine Kinase
RTKi	Receptor Tyrosine Kinase inhibitor
RT-PCR	Real time polymerase chain reaction
SD	Standard deviation
SDS-PAGE	Sodium dodecylsulphate polyacrylamide gel electrophoresis
SH2	Src Homology 2
siRNA	Small Interfering RNA
STAT	Signal Transducer and Activator of Transcription
TBS	Tris buffered saline
TBS-T	TBS with 0.1% Tween-20
TGF	Transforming Growth Factor

List of Figures

Chapter 1: Introduction

Chapter 3: Results

Chapter 4: Discussion

List of Tables

Chapter 1: Introduction

1.1 Head and Neck Squamous Cell Carcinoma: History and Biology

Squamous cell carcinoma of the head and neck (HNSCC) is the sixth most common cancers in the world and it accounts for approximately 90 % of the cancers that occur in the mucosa of the head and neck (1). The risk of developing this type of cancer increases with the use of tobacco and alcohol (1). Furthermore, it has been found that Human Papilloma Virus (HPV) is a risk factor for HNSCC (2). Presently, localized HNSCC tumors are treated with radiation or surgery (3); however, in advanced cases either radiation or surgery is generally combined with chemotherapy (4). Unfortunately, long-term survival remains relatively unchanged despite advancements in the fields of surgery, therapeutic agents and radiation delivery (5) and thus new therapeutic options are required in order to increase over-all survival of patients with HNSCC. In order to identify superior alternative treatments, we need to improve our understanding of the biology of this cancer.

Studies have shown that the Epidermal Growth Factor Receptor (EGFR) is directly associated with HNSCC and plays a major role in their pathogenesis, in fact EGFR is up-regulated in 90% of these tumors (6, 7). A variety of studies have demonstrated that higher levels of expression of EGFR are linked to poor prognosis (8-10). This makes EGFR a suitable target for the development of more efficacious therapies. Preclinical studies that target the EGFR in HNSCC models have shown promising results (11, 12); however, even though the EGFR is targeted using different methods, downstream signalling pathways are often deregulated leading to resistance to these agents (13). For example, cross-talk between the EGFR and other growth factor receptors such as the Insulin Growth Factor Receptor (IGFR) and G-Protein Coupled Receptors (GPCR) can maintain proliferative and survival

signals in these cells (14). Thus, targeting the EGFR in combination with other strategies, like radiation or other drugs that show activity in HNSCC, may represent a superior approach. A more expansive knowledge of EGFR functions, its effectors and downstream pathway regulations will lead to strategies to improve the effectiveness of this class of agents in cancer therapy.

1.2 The Epidermal Growth Factor Receptor Structure and Function:

The epidermal growth factor receptor (also erbB1, HER1) is the most studied protein of the ErbB family of receptor tyrosine kinases (RTK). It was first purified by Cohen et al in 1980 (15). EGFR is a 170 kDa glycoprotein encoded by a gene at the 7p12 locus (16). It consists of an extracellular ligand-binding domain, a lipophilic trans-membrane domain and an intracellular domain that contains the kinase activity and key tyrosine residues involved in trafficking and binding of adaptor proteins and downstream effectors that contain an SH2 domain (Figure 1.1) such as phospholipase C, for example (17, 18). The ectodomain of the receptor is comprised of four domains; two of them are involved in binding the ligand and two cysteine rich domains involved in dimerization. These domains are arranged in an alternating fashion from the N- to the C-terminus as follows: L1-CR1-L2-CR2 where the ligand binding site including L1 and L2 are designated domains I and III and the cysteine rich segments are designated domains II and IV (19). Ligands that activate EGFR signalling include the Epidermal Growth Factor (EGF), Transforming Growth Factor alpha (TGF-α), amphiregulin and Heparin-Binding EGF-like Growth Factor (HB-EGF) (20). Each ligand allows for dimerization with a different partner and propagates a signal via a different pathway which allows for horizontal amplification and diversification of the signal (21).

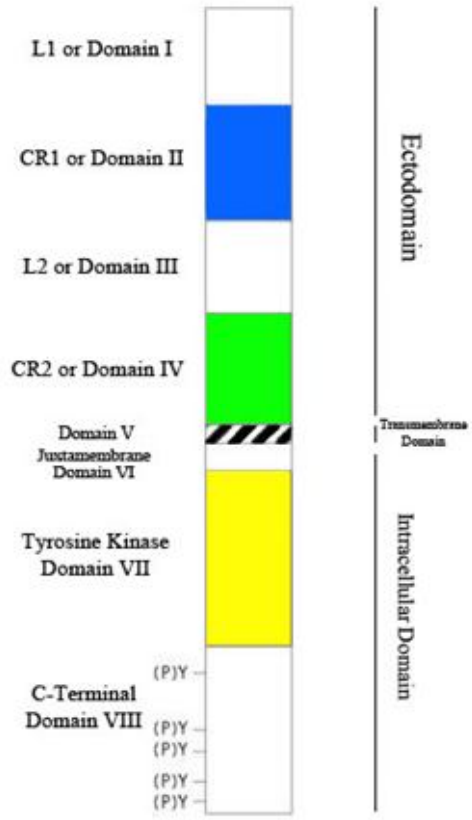

Figure 1.1. Domains of the Epidermal Growth Factor Receptor. The EGFR is composed of an extra-cellular ligand-binding domain (Divided into Domains I,II,III and IV), a trans-membrane domain (Domain V), and an intracellular domain with kinase activity (Domains VI,VII and VIII) and key tyrosine residues that play a major role in signal transduction.

Moreover, the EGFR has been shown to be activated by a multitude of other signals from integrins (22), membrane depolarization (23), cellular stress (24) and G-protein-coupled receptors (25, 26). In the absence of an activation signal, the EGFR exists in an equilibrium state between auto-inhibited tethered conformation (~95% of total EGFR) in which domain II is buried into domain IV by virtue of intramolecular interactions and an untethered conformation (~5%) (Figures 1.2 A and B). Its ligands bind to domains I and III stabilizing the receptor in the extended or untethered form and exposing the cysteine-rich dimerization arm of domain II that is crucial for dimerization to occur (27, 28) leading to a rightward shift of equilibrium according to the classical Le Cahtelier's principle of chemical equilibrium. Following this change in conformation, the EGFR can homo- or hetero-dimerize with any of the ErbB family members, preferentially ErbB2, and it is at this point that the receptor's kinase domain becomes activated (27) (Figure 1.2 C) leading to phosphorylation of key tyrosine residues in the C terminal intracellular domain of the receptor as well as phosphorylation of many cytoplasmic substrates (29, 30). After that, the ligand-receptor complex is internalized in endosomes where one of two events can occur, the EGFR will either be recycled to the cell surface or targeted to lysosomes for degradation. It is now well established that activated EGFR signals through major pathways: the Ras-Raf-MAPK, PI3K-Akt, Jak-Stat, and PLC-gamma (7, 31, 32) that mediate signals implicated in a myriad of pro-survival cellular functions ranging from proliferation, to differentiation, motility, protein synthesis and DNA repair (Figure 1.3) (31, 33, 34). In addition to its traditional role as a signal transducer across the cytoplasmic membrane, the EGF receptor has also been found to localize to the nucleus (35, 36). In the nucleus the receptor is thought to directly bind DNA promoter regions or as part of a transcription initiation factor complex, activating pro-survival genes resulting in cancer resistance and poor patient prognosis (37-39).

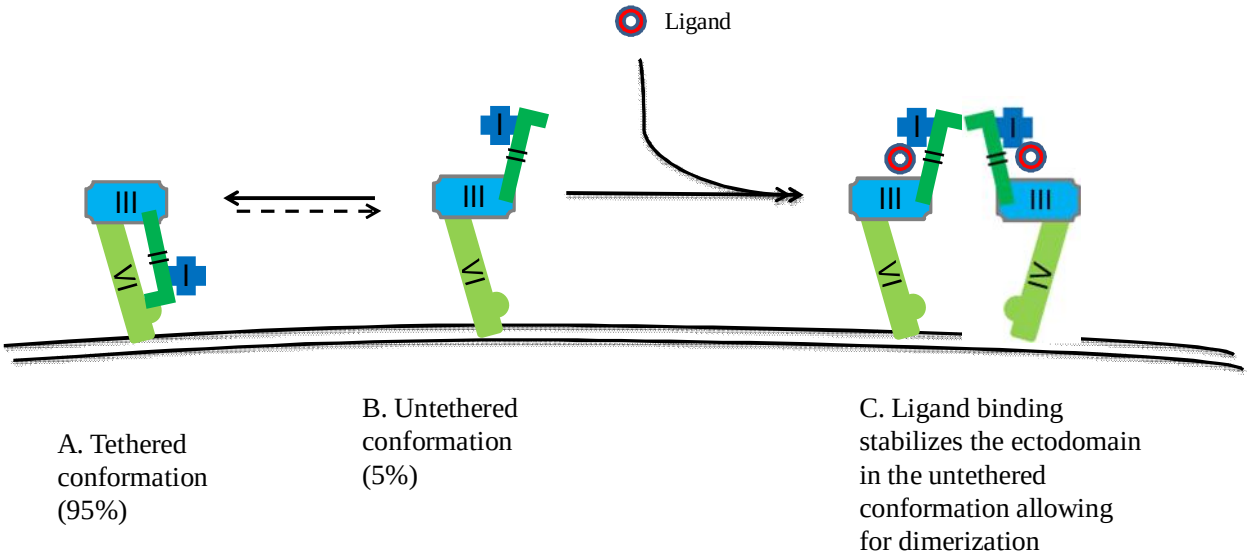

Figure 1.2. Ligand-Induced EGFR Dimerization. **(A)** Unliganded EGFR exists in a tethered conformation, in which domains II and IV form an intramolecular interaction (95%) or **(B)** in an untethered form. **(C)** Ligand binds and interacts simultaneously with domains I and III, stabilizing the extended form which exposes domain II and the receptor can dimerize. Domain II from two ligand-stabilized receptors interact forming an activated dimer. Adapted from Li et al. 2005.

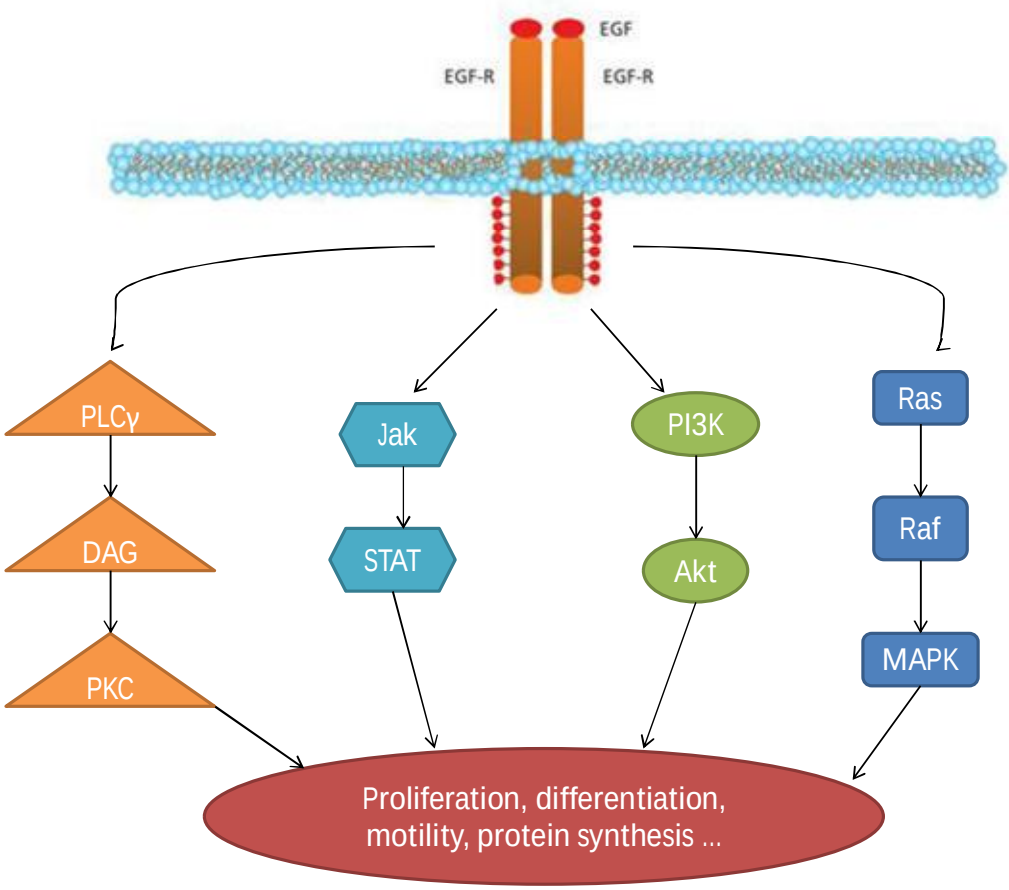

Figure 1.3. Major EGFR Signalling Pathways. The EGFR sits on the apex of versatile signalling pathways that regulate vital cellular processes such as proliferation, differentiation, motility, protein synthesis and DNA repair.

Therefore, many extracellular signals converge on the EGFR which in turn regulates a multitude of vital cellular processes. Furthermore, the EGFR has been implicated in the regulation of growth, proliferation, aggressiveness and therapy resistance of many cancers including HNSCC (32). These facts further support the rationale for focusing on this important RTK as a target for cancer therapy.

1.2.1 EGFR Targeted Therapies:

Various strategies have been implemented to target the EGFR at different stages of its signalling cascades and its expression. The most clinically advanced strategies are monoclonal antibodies (MAbs), receptor tyrosine kinase inhibitors (RTKi), antisense oligonucleotides and siRNA-mediated blocking of its transcription, and ligand-toxin conjugates.

1.2.1a Monoclonal Antibodies:

Monoclonal antibodies function by targeting the extracellular ligand domain of the EGFR and compete with the native ligands (40, 41). Many antibodies have been raised against different EGFR epitopes, but they all exert their effects by preventing ligand binding to the receptor, or prevent receptor dimerization due to steric hindrance resulting in abrogation of kinase activity and preventing signal transduction (42, 43). Furthermore, it has been shown that antibody binding results in increased internalization and lysosomal degradation of the receptor (44). On the other hand, MAbs can also enhance the function of the immune system via opsonisation of cancer cells. As studies have shown antibodies enhance targeting of the cancer cells by natural killer cells and dendritic cells in HNSCC in vitro (45, 46). Due to all these effects, antibody based therapies are being extensively used

clinically. For example, cetuximab (C255, erbitux), a chimeric mouse-human IgG antibody was approved by the Food and Drug Administration (FDA) in 2006 to be used with radiation therapy for treatment of HNSCC as it was demonstrated that combining radiation with cetuximab increased the duration of overall survival to 49 months compared to 29.3 months with radiation alone (47).

1.2.1b Antisense Oligonucleotides and siRNA:

Antisense oligonucleotides are short segments of single stranded DNA molecules that can range between 20 to 25 nucleotides in length that exert their effect by targeting the sequence of messenger RNA of a specific gene. This acts to prevent its translation by sterically hindering the binding of the ribosomal subunits thus ceasing translation of the transcript to protein (48). siRNA are double stranded RNA molecules that contain a sequence corresponding to the target gene to be silenced (49). Its mechanism of action is very different from antisense oligonucleotides but they both aim to target a gene at the level of mRNA translation. Once inside the cell, siRNA is cleaved by an enzyme named Dicer creating a 20 bp double stranded RNA molecule (50). Those then bind to RNA-induced silencing complex (RISC), unwind, and are then carried to the target mRNA to be silenced by RISC (51). Finally, slicer, which is part of the RISC complex, enzymatically excises the transcript mRNA in question (52). Both of these strategies have shown promising pre-clinical results. For example, a study that employed antisense oligonucleotides to treat xenografted squamous cell carcinoma demonstrated a significant reduction in tumor burden, lower EGFR expression levels and increased tumor cell apoptosis when compared to vector treated controls (53). Another study using siRNA targeting EGFR transcripts to treat HNSCC

xenografts showed similar results, and when used in combination with cisplatin the treatment was improved (12).

1.2.1c Antibody/Ligand-Toxin Conjugates:

Another strategy to target the EGFR is with antibody- or ligand-toxin conjugates. The rationale behind this strategy is to deliver a toxin, extracted from bacteria such as diphtheria or pseudomonas, directly and specifically to tumor cells that overexpress EGFR. Delivery of these toxins to the cytoplasm of the cell by endocytosis leads to ADP ribosylation of the eEF2 leading to cessation of protein synthesis (54). Studies have used this strategy to treat HNSCC, and other types of cancers with upregulated EGFR expression, in vitro and in vivo and have shown promising results. One such study has demonstrated that treatment of a glioblastoma xenograft model with TGF-alpha conjugated to the PE38 toxin (a modified pseudomonas toxin) showed tumor growth delay and regression (55). Another study used the same ligand-toxin conjugate in a HNSCC cell line model and xenografts and showed that cleaved PARP, which is a marker of apoptosis, is significantly higher in the treated groups versus control (56).

1.2.1d Receptor Tyrosine Kinase Inhibitors:

This class of therapeutic agents consists of low molecular weight inhibitors that act on the intracellular kinase domain of the EGFR and compete with and reversibly bind to the ATP binding site at K745 (57) preventing the trans-autophosphorylation of the receptor and subsequently abrogating the downstream signal transduction. Two anilinoquinazolines, Gefitinib (ZD 1839, Iressa®) and Erlotinib (OSI 774, Tarceva®), are examples of RTKi's that have been approved by the FDA for the treatment of Non Small Cell Lung Carcinoma

(NSCLC) in 2003 and 2004, respectively. They are active, orally available drugs which make them a more attractive alternative to the IV-introduced MAbs. Initial Phase I clinical trials with these agents showed promising clinical activity (58, 59) in a variety of cancers which led to further investigations. In Phase II trials on patients with NSCLC; a response rate ranging from 10% to 18% was reported for gefitnib (60, 61). However, a follow-up series of Phase II trials were conducted and these RTKi's failed to increase survival when combined with classical chemotherapy (62, 63). In 2005, Shepherd and coworkers conducted a Phase II clinical trial on NSCLC patients that had already received first- or second-line chemotherapy and demonstrated that erlotinib as a single agent improved patient survival compared to placebo (64). Clearly there is a need to enable better identification of patients who would benefit from this type of treatment and uncover novel therapeutic combinations of these agents to enhance their efficacy. Interestingly, recent studies have revealed that a subset of NSCLC patients respond more robustly to treatment with these drugs due to the presence of mutations in exons 18 to 21 encoding the kinase domain of the EGFR (65, 66). These mutations are believed to stabilize ATP binding conferring enhanced activity to this mutated receptor, however, the TKi also show enhanced binding to the ATP binding pocket rendering tumor cells with these mutations more sensitive to these agents (66).

1.3 Mechanisms of Resistance to Therapy:

Over the past decade there has been significant development and diversity in the field of cancer therapy; however, the increase in survival of cancer patients with HNSCC, or any of the other cancers that overexpress the EGR, has been very modest. This is largely due to the development of resistance to the treatment modalities mentioned above, especially when prescribed as monotherapy. Indeed, the ability of cancer cells to adapt is the treatment obstacle that must be overcome to produce durable patient responses and cures.

The need to develop novel therapeutic options stems from the fact that classical therapies such as chemotherapy and radiation are less affective as the disease progresses. The ability for cancer to repopulate rapidly between sessions of fractionated radiotherapy is one of the main causes of resistance. In the case of EGFR targeted therapies, multiple resistance mechanisms can be activated against MAbs effects as targeting of EGFR by cetuximab induced up-regulation of Her2 and Her3 and their downstream signalling as a compensatory mechanism (67). Resistance to TKi's occurs as a result of mutations in the internal ATP-binding domain. A common mutation that confers resistance to gefitinib and erlotinib in NSCLC is a T790M substitution that changes the conformation of the ATP binding site lowering the binding affinity of these drugs (68). Moreover, increased expression of c-Src can also confer resistance to erlotinib by activating c-Met (69). Stabile et al. developed a HNSCC cell line that overexpresses activated c-Src and observed that c-Src expressing cells are about four times more resistance to erlotinib than the vector control (69). Furthermore, activated c-Src increases c-Met phosphorylation and activation, and that inhibition or knock-down of c-Met sensitizes these resistant clones to erlotinib both in vitro and in vivo (69). Inhibition of the EGFR is a promising therapeutic approach that holds potential as a treatment option for patients with HNSCC; however, identifying patients that will likely benefit from this approach, overcoming drug resistance and identification of combination based therapies to enhance efficacy are major hurdles limiting the progress of this strategy.

1.4 Statins in Cancer Therapy:

Statins are a class of drugs that are widely prescribed to patients with high plasma cholesterol levels to reduce the risk of cardiovascular disease. Mevinolin, currently known as lovastatin (Figure 1.4), was the first statin discovered and was an extract from the fungus Aspergillus terreus (oyster mushrooms). This drug was found to potently inhibit the enzyme

3-hydroxy-3methylglutaryl-coenzyme A (HMG-CoA) reductase in rats and dogs resulting in a significant decrease of plasma cholesterol levels (70). HMG-CoA reductase is the rate limiting enzyme in the mevalonate pathway, which is an important metabolic pathway that produces a variety of metabolites that are essential for a multitude of cellular processes and structures (71). The end products of the mevalonate pathway include cholesterol, heme A, ubiquinones, dolichol, farnesyl pyrophosphate (FPP) and geranylgeranyl pyrophosphate (GGPP) (71). The cell uses cholesterol to control the fluidity of their membrane and in the synthesis of new cytoplasmic membrane during cell division as well as in the formation of steroid hormones (71). Heme A is a component of hemoglobin and cytochromes. Ubiquinone, otherwise known as co-enzyme Q10, is an important component of the inner mitochondrial membrane that participates in the electron transport chain and the formation of ATP (71). Dolichol is an important carrier molecule for oligosaccharides that aids in the synthesis of glycoproteins (71). And finally, FPP and GGPP are isoprenoid molecules that are used in the post-translational modification of certain proteins especially the Ras superfamily of small GTP-binding proteins (72). The addition of these 15 to 20 carbon molecules to their c-terminus provides these proteins with a membrane anchor allowing for their proper cellular localization that is critical for their function (73, 74). The GTPases hydrolyse GTP to GDP and trigger signal transduction pathways and are central regulators of cellular proliferation, trafficking, motility and survival (Figure 1.5) (75).

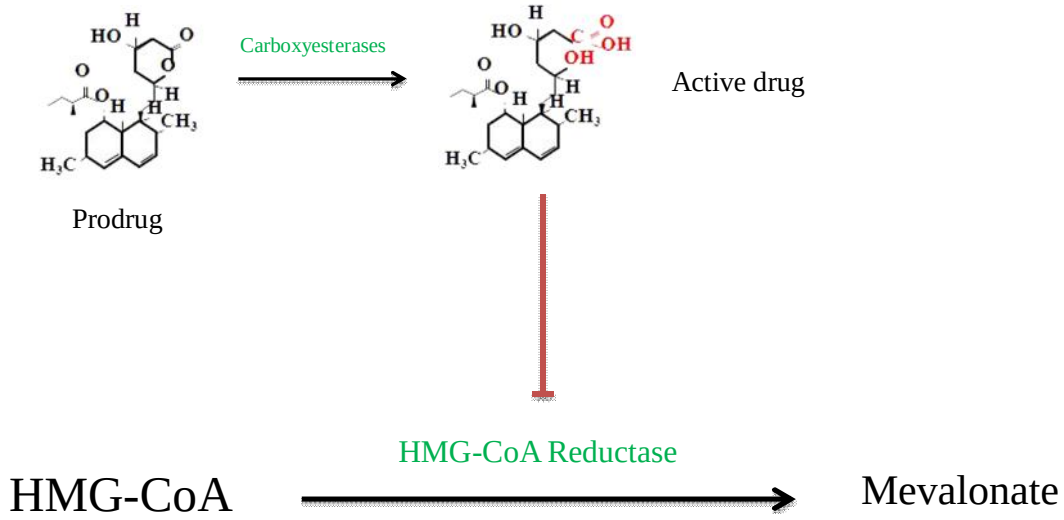

Figure 1.4. Inhibition of Mevalonate Production by Lovastatin. Lovastatin is activated by carboxyesterases in the plasma and liver giving the molecule a carboxylic group. In that form lovastatin resembles an intermediate that has a 1000x more affinity to the HMG-CoA reductase than its natural substrate which, upon binding to the enzyme, inhibits the conversion of HMG-CoA to mevalonate.

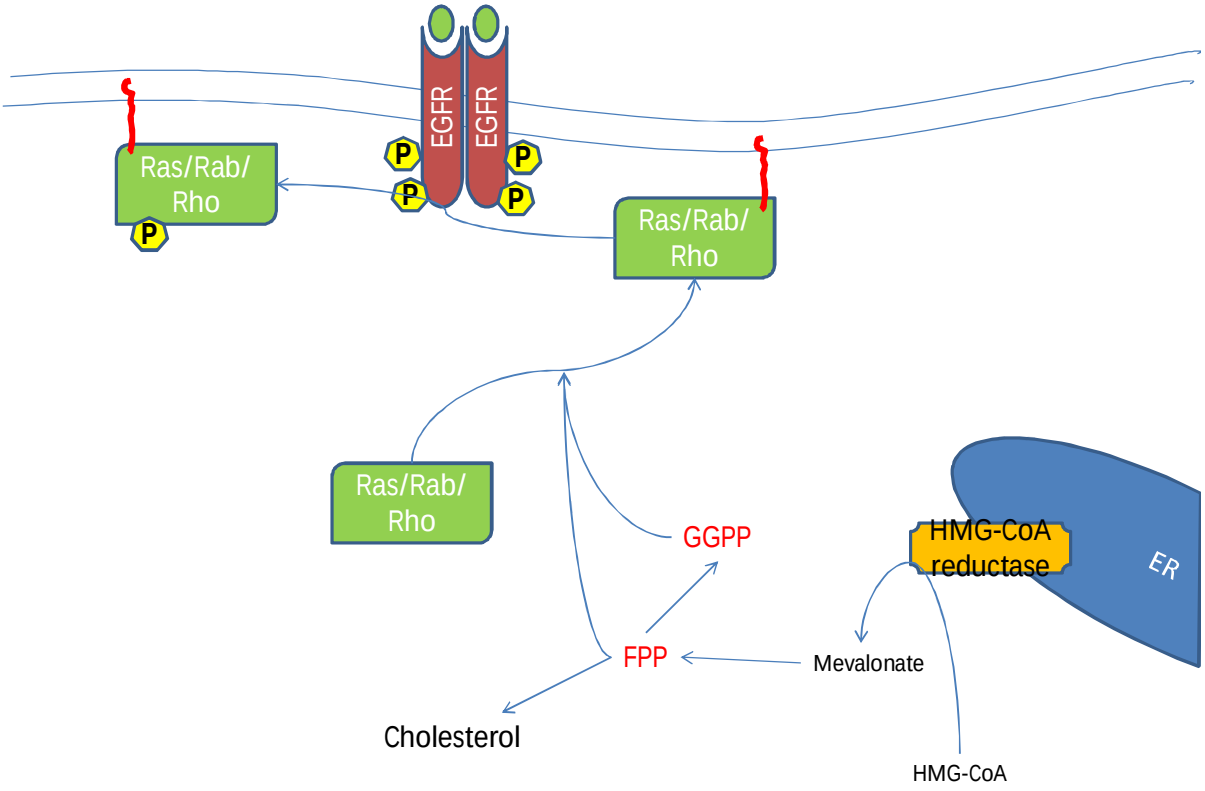

Figure 1.5. The Mechanism Linking the Mevalonate Pathway, Ras, and the EGFR.

This figure explains how the mevalonate pathway is connected to regulation of EGFR signalling through GTPases such as Ras. Production of farnesyl pyrophosphate (FPP) in the mevalonate pathway is required for prenylation of the Ras protein which targets it to the cytoplasmic membrane in close proximity to the EGFR. Ligand binding to the EGFR leads to activation of Ras that switches on downstream effectors.

The Ras superfamily of proteins, including Rho and Rab, have been implicated as playing roles in the pathogenesis of a multitude of cancers. Since prenylation is an essential post-translational modification for the functionality of these proteins, statins have been studied as a potential anti-cancer therapeutic approach. In the 1990's clinical trials investigated the tolerability of lovastatin in cancer treatment, and concluded that this statin is well tolerated at high doses with the limiting dose being myopathy that was reversed by ubiquinone supplementation in about 60% of the patients (76, 77). Further studies using lovastatin on a wide variety of cancer cell lines revealed that lovastatin is a potent inducer of apoptosis in cancers from different origins such as juvenile monomyelocytic leukemia, rhabdomyosarcoma, medulloblastoma, and squamous cell carcinoma of the cervix and of the head and neck (78, 79). These studies clearly demonstrate the dependency of certain types of cancer on the end products of the mevalonate pathway, since their depletion through inhibition of HMG-CoA reductase caused a marked decrease in viability of multiple cancer cell lines in vitro. These findings led to a phase I clinical trial of lovastatin, as a single agent, in patients with recurrent or metastatic head and neck or cervical squamous cell carcinoma where 23% of patients showed stable disease for 3 months (80).

1.5 Receptor Tyrosine Kinase Inhibitors and Lovastation: A Rational Combination

It is now well documented that GTPases of the Ras super family of proteins regulate the transduction of signal via the EGR. For example, the Ras protein is part of the classical pathway comprising EGFR→GRB2→RAS→Raf→MEK→ERK (81, 82); and along with other members of the family such as the Rab, Rho and Rac regulate the RTK activity on a myriad of vital cellular functions like proliferation survival, motility and intracellular trafficking (72, 83). Therefore, any disturbance in the function of these GTPases will lead to

disruption in the signalling cascade by EGFR (Figure 1.5). Based on this theory, our laboratory combined lovastatin with gefitinib, a clinically advanced small molecule EGFR inhibitor (84). Lovastatin treatment through preventing prenylation of the GTPases may affect the EGFR pathway and activation, and enhance gefitnib efficacy. It is important to note that inhibition of the mevalonate pathway by lovastatin does not inhibit formation of the FPP and GGPP directly and thus depletion of these metabolites requires time thus the reason why we pretreat cells with lovastatin before combining with RTKi's. Indeed, combining lovastatin with gifitinib resulted in a synergistic and potent apoptotic response in a panel of NSCLC and HNSCC derived cell lines (84); moreover, lovastatin inhibits ligand induced EGFR and AKT activation (84). Additional studies in our laboratory revealed that lovastatin was able to inhibit EGFR dimerization, an effect that was regulated by lovastatin's ability to target the cytoskeleton through targeting the rho proteins (85), which confirms the link between the mevalonate pathway and EGFR signalling. These findings led to the initiation of a Phase I/II trial at the Ottawa Hospital to assess the potency of combining rosuvastatin and erlotinib in patients with NSCLC. Completion of the Phase I component resulted in determination of the suitable dose and demonstrated the potential of clinical activity; however, as a consequence of high statin dose used in this study a high incidence of myopathy limited the use of this approach.

As a result, the next logical step in the progression of the strategy was to either lower the dose of statins used or to replace statins with another agent that will similarly sensitize tumors to RTKi's without the associated side effects. To achieve this end, we conducted a high throughput screen employing a Prestwick Library of 1200 compounds all of which have FDA approval for a wide variety of indications. A screen of this library at a concentration of 1 μM for each compound in combination with either 10 μM lovastatin or erlotinib on two

HNSCC cell lines SCC25 and SSC9 and a lung cancer cell line A549 was performed. The goal of this screen was, ideally, to find an agent that would not be cytotoxic on its own but would augment the cytotoxicity of both lovastatin and erlotinib. This screen produced seven hits that enhanced the efficacy of lovastatin, and nine hits that enhanced the efficacy of erlotinib (Table 1.1). Some of the hits were expected and confirmed the previous work done in our laboratory such as the identification of RTKi's as hits in the lovastatin combination screen and, vice-versa, the appearance of statins as hits in the erlotinib screen. In addition to the expected result, two drugs, colchicine and monensin, were able to enhance the potency of both lovastatin and erlotinib (Dimitroulakos J. et al., unpublished data). The studies outlined in this thesis focus on the drug monensin in an attempt to characterize its ability to improve the anti-cancer effects of lovastatin and erlotinib.

Lovastatin-enhancing Hits				
EGFR Inhibitors	**Cardiac Glycoside**	**Chemotherapies**	**Microtubule Polymerization**	**Block Protein Transport**
gefitinib	lanatoside	daunorubicin	colchicine	monensin
erlotinib		doxorubicin		
Erlotinib-enhancing Hits				
Mevalonate Pathway	**Anti-Metabolites**	**Chemotherapies**	**Microtubule Polymerization**	**Block Protein Transport**
fluvastatin	methotrexate	gemcitabine	colchicine	monensin
alendronate	floxuridine	doxorubicin		
		etoposide		

Table 1.1. High Throughput Prestwick Library Screen Hits. Drugs that enhance the cytotoxicity of lovastatin are shown in the upper part of the table whereas erlotinib-enhancing drugs are displayed in the lower part.

1.6 Monensin: From Farms and Ranches to Cancer therapy

Coccidiosis, a parasitic infection, was a major problem facing the poultry industry in the 1940s until the introduction of sulfaquinoxaline to the feed (86); however, resistance rapidly became an issue. In 1967 Agtarap et al. described the structure of monensic acid, now known as monensin, and it was reported to be an effective anti-coccidial agent (87).

Furthermore, it was subsequently reported that monensin also promotes muscle weight gain and milk production in cattle (88). As a result, it is the most widely used product of its kind in farms in the United States. Monensin is an antibiotic secreted by the bacteria Streptomyces cinnamonensis and classified as a polyether antibiotic or ionophonre which is a term chosen that means "ion bearer" (89). Monensin has the molecular formula $C_{36}H_{62}O_{11}$ (Figure 1.6A), it forms a cyclic conformation where the oxygen atoms form a circle around certain cations (Figure 1.6 B) while the alkyl groups protrude making the molecule highly lipid-soluble. This allows monensin to freely pass across the lipid bilayer of the cytoplasmic membrane or cellular organelles transporting ions along by passive diffusion (90). Biologically relevant ions that can be chelated by monensin are $Na^+ > K^+ > Ca^{2+}$ with a 10 fold higher affinity towards sodium than potassium (91). During ion transport, monensin crosses the lipid membrane, loses the proton on the carboxylic group and chelates a cation then it crosses back to the opposite side of the membrane losing the ion in exchange for a proton and the cycle repeats (89). The mechanism by which monensin inhibits coccidiosis has been the subject of debate and many groups have suggested different theories to explain that phenomenon. Estrada et al. found that this drug inhibits potassium ion transport into the mitochondria from rat liver leading to inhibition of energy production (92) and it was proposed as a mechanism that takes place in coccidial mitochondria although there has been no evidence to support this claim (93). Another group suggested that monensin causes excess sodium ion accumulation inside the sporozoite leading to continuous activation of the Na^+/K^+ pump, a process that consumes a lot of energy thus diverting the use of ATP from anabolic mechanisms and growth towards ion gradient regulation mechanisms (94). Furthermore, high sodium concentrations inside the parasite causes water retention by osmosis leading to swelling of the coccidian and eventually bursting (94).

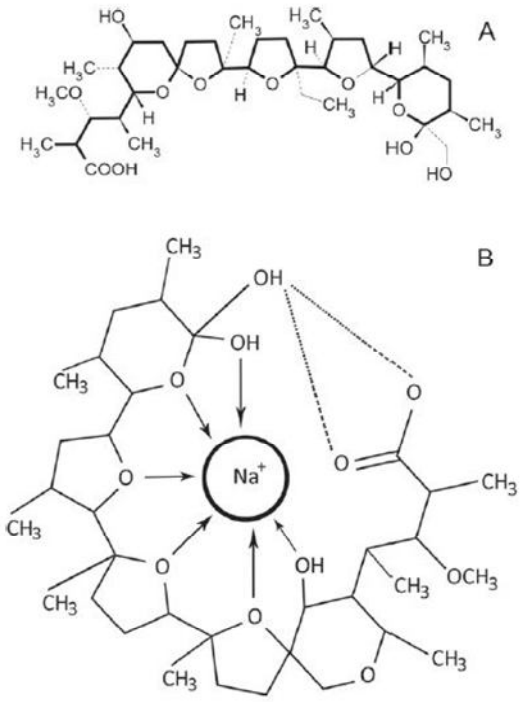

Figure 1.6. The Chemical Structure of Monensin A. **(A)** The free form of monensin not bound to a cation. **(B)** The cyclic form of monensin chelating a sodium cation. Adapted from Chapman et al. 2010.

Further study of the ionophore revealed that monensin disturbs the localization of a protein called flotillin-1 in lipid rafts found at the apex of the coccidia which is a region important for host cell invasion, this constitutes yet another mechanism of function of monensin (95).

During the past decade or so, monensin has been the focus of many cancer research laboratories and it has successfully shown effectiveness in targeting cell lines derived from many cancer types, including renal cell carcinoma (96), colon cancer (97), myeloma (98), lymphoma (99), prostate (100) and others. Furthermore, Ketola et al. compared the cytotoxic effect of monensin between malignant versus non-malignant cell lines and concluded that non-malignant cell lines are more than 20 fold more resistant than their malignant counterparts (100). Park et al. demonstrated that monensin displays its effect on cells by inhibiting different cyclins and cyclin dependent kinases, depending on the cell line, and induces apoptosis by disrupting the mitochondrial membrane potential and activating caspases among other apoptotic indicators (96-99, 101). On the other hand, monensin seems to have different effects on prostate cancer derived cell lines as reported by Ketola and colleagues. According to them, monensin leads to down regulation of androgen receptor resulting in androgen withdrawal (100) which has been shown to induce apoptosis in prostate cancer (102). In addition, this antibiotic was able to inflict oxidative stress damage, which was reversed by the addition of vitamin C to the culture, and inhibit aldehyde dehydrogenase activity leading to aldehyde-induced oxidative stress and therefore apoptosis (100). Monensin has, according to the mentioned literature, proven to be a potent and cancer-specific, in the case of prostate cancer, agent. Furthermore, it has been shown to have a positive safety profile in veterinary medicine since it has been used in cattle and poultry feed for the past four decades or so. This has made monensin an attractive agent that opens a new

avenue for investigation as a cancer treatment especially since esters of monensin can be synthesized by adding different reactive groups to the carboxylic acid moiety resulting in different biological activities and perhaps diminishing side effects (103).

2. Rationale, Hypothesis and Objectives

Tumor ability to adapt and develop erlotinib resistance, and resistance to RTKi's in general, has been a persistent problem and a major drawback in targeting the EGFR in cancer therapy. Therefore, the need to find a means to counter this problem is imperative. Our laboratory has previously identified lovastatin as an agent that augments the efficacy of gefitinib and has extensively investigated the effect of statins on cancer biology and metabolism in order to identify novel therapeutic strategies and targets (84, 85, 104). These studies eventually led to clinical trials that showed disease stabilization, although the high dose of statins used had undesirable effects on a significant number of patients, which called for an alternative approach to improve cancer targeting while at the same time minimizing the side effects of the treatment regimen. High throughput analysis of 1200 compounds in combination with lovastatin or erlotinib lead to the identification of monensin as a potent enhancer of their cytotoxicity in two HNSCC (SCC9 and SCC25) derived cell lines and a lung adenocarcinoma derived cell line (A549) (Dimitroulakous et al. unpublished data). In the work proposed in this thesis, we aim to confirm the effect exhibited upon combining monensin with lovastatin or erlotinib in an attempt to identify new therapeutic approaches with minimal adverse side effects.

Hypothesis

Monensin synergistically augments the cytotoxicity, when combined with lovastatin or erlotinib, through further targeting of the EGFR.

Objectives

1- To validate monensin as a sensitizing agent to lovastatin- and erlotinib-induced cytotoxicity in HNSCC cell models.

2- To evaluate the effect of monensin on EGFR activation, trafficking and downstream signalling and identify monensin targets.

3- To assess the potency of monensin in ex-vivo tumor samples from patients with HNSCC.

Chapter 2: Materials and Methods

2.1 Cell Culture

HNSCC cell lines SCC9 and SCC25 and normal lung fibroblasts WI38 cell lines were purchased from American Type Culture Collection ATCC (Rockville, MD). SCC9-R4 clonal sub-line is a lovastatin resistance clone developed by prolonged exposure to a high concentration of lovastatin (10 µM for 28 days) and cloned through single cell dilution. Cells were grown and maintained in Dulbecco's modified Eagle's medium (DMEM) (Cellgro, Manassas, VA, USA) supplemented with 1% (v/v) penicillin/streptomycin (Sigma Aldrich, St Louis, MO, USA) and 10% (v/v) fetal calf serum (Hyclone). Incubation settings were maintained at 37ºC and 5% CO_2. SCC9 and SCC25 are good HNSCC cell models because they overexpress wild type EGFR.

2.2 Drugs

Erlotinib (Tarceva) hydrochloride was purchased from BioVision (Mountain View, CA) and resuspended and diluted to 10 mM stock in dimethyl sulfoxide (DMSO). Lovastatin was obtained from Apotex (Toronto, ON) and suspended in ethanol to 10 mM. Sodium salt

of monensin was purchased from Sigma-Aldrich (St Louis, MO, USA) and suspended in ethanol to 10 mM solution.

2.3 Western Blots and Densitometry

SCC9 and SCC25 cells were pretreated with 0, 0.1 or 1 µM monensin (Sigma-Aldrich, St-Louis, USA), for 22 hours followed by 2 hours treatment with control, 10, 1, 0.1, 0.01 and 0.001 µM erlotinib in serum free media. Cells were then stimulated for 15 minutes with 50 ng/ml Epidermal Growth Factor (EGF) before lysis with RIPA buffer (50mM Tris-Cl, 150mM NaCl, 1mM EDTA, 1% (v/v) Triton X-100, 0.25 % (w/v) sodium deoxycolate and 0.1% (w/v) SDS and pH 7.5) supplemented with protease inhibitor cocktail (Sigma Aldrich), 17.5 mM beta-glycerophosphate and 0.2 mM Na_3VO_4 (Sigma-Aldrich, St-Louis, MO, USA). The samples' protein contents were quantified using the Pierce BCA protein assay protocol (Pierce, Rockford, IL, USA) and absorbance read on a BioTek Synergy MX plate reader and analyzed using Gen5 software (BioTek, Winooski, VT) at 562 nm. Samples were then resolved by SDS-PAGE, transferred onto polyvinylidene fluoride membranes (Immobilon-P, Millipore, Billerica, MA, USA). Blocking the membrane was performed with 5% BSA (Bovine Serum Albumin) (Sigma-Aldrich) in Tris-Buffered Saline with 0.1% Tween-20 (TBS-T) and Western blotted with the following primary antibodies: EGFR, Akt, pAkt, ERK, pERK (Cell Signalling Technology, Davers, MA, USA) overnight at 4C and diluted 1/1000, pY20 (BD Biosciences) overnight at 4°C and diluted 1/2000, and actin antibody (Sigma Aldrich) for 1 hour at room temperature and diluted 1/10000. Dilution of antibodies was made in 5% BSA 0.1% TBS-T. Blots were washed twice with 0.1% TBS-T and once with TBS for 5 minutes each wash, then incubated for 1 hour at room temperature with the appropriate HorseRadish Peroxidase (HRP)-tagged secondary antibody (anti-rabbit

1/2500 and anti-mouse 1/300 Jackson ImmunoResearch, West Grove, PA, USA). Supersignal west pico chemiluminescence substrate (Pierce) was applied to the blot and developed using Syngene bioimaging system (Syngene Bio-imaging, Frederick, MD).

Densitometric analysis was performed using the GeneTools software from Syngene (Syngene Bio-imaging). The density of the non-phosphorylated EGFR antibody was normalized with that of the actin antibody, then the density of the pY20 antibody of the 170 kDa band was divided by the normalized density of the non-phosphorylated EGFR and taken as percentages. This was done in triplicates to obtain a SD error bar.

2.4 (4,5-Dimethylthiazol-2-yl)-2,5-Diphenyltetrazolium Bromide (MTT) Assay

SCC9, SCC25 and WI38 cell lines were seeded on 96-well flat-bottomed plates (Corning Costar #3595, Corning, NY, USA) in 75 ul/well. Cells were seeded at different densities (previously determined by optimization) due to variation in doubling rates and differences in metabolic activity. The cells were left to incubate overnight at 37 °C and 5% CO_2 to allow for attachment and recovery. On the next day, cells were pretreated with lovastatin (0, 1, 5, or 10 µM) to treat with monensin on the next day (0-25 µM) or monensin (0-25 µM) to treat with erlotinib after 24 hours (0, 1, 5 and 10 µM). Drugs were prepared at 2X concentration in 75 µl and added to the plates already containing 75 µl of media for a final volume of 150 ul. Twenty four hours later, the media were removed and replaced by pretreatment drugs and an increasing concentration of monensin (0, 0.1, 0.5, 1, 2, 5, 10, 25 µM) in the case of lovastatin pretreated cells and erlotinib (0, 1, 5 and 10µM) in case of monensin pretreated cells in a final volume of 150 µl of fresh media.

After 48 hours, 5 mg/ml in 42 µl of MTT reagent (Sigma-Aldrich) dissolved in phosphate buffered saline (PBS) was added to the cells, which were then incubated at 37 °C in the dark

for 2 hours. HCl (84 µl of 0.01N) in 10% sodium dodecyl sulphate (SDS) was added to cells and incubated at 37ºC for 24-72 hours to lyse the cells. MTT activity was measured by reading absorbance at 570 nm using a BioTek Synergy MX plate reader and analyzed using Gen5 software (BioTek, Winooski, VT). Cellular viability was assessed relative to a blank column of wells, which contained no cells and thus represents no viability, and an untreated column which represents healthy cells.

Note: Not all data points are presented in the figures as higher concentrations of drugs had a high toxic effect, especially with the combinations, and thus data (on the x-axis) was limited to certain concentrations to make figures presentable.

2.5 RNA isolation and RT-PCR from cell lines

SCC25 and SCC9 cell lines were treated with either 1 µM monensin or control for 24 hours and then the total RNA content was extracted using the RNease® kit (Qiagen, Germantown, MD, USA) following the manufacturer's protocol. The concentration of RNA was quantified using Take3 Micro-Volume plate and BioTek Synergy MX plate reader and analyzed using Gen5 software (BioTek, Winooski, VT). 1 µg of total RNA was used for reverse transcription to cDNA using a High Capacity cDNA reverse transcription kit (Applied Biosystems) according to the manufacturer's protocol in an ABI Thermal Cycler (Applied Biosystems, Foster City, USA). The synthesized cDNA was used to carry out real-time polymerase chain reaction (RT-PCR). The total reaction volume of 20 µl contained 2 µl of cDNA, 1 µl TaqMan Gene Expression Assay Primer/Probe (20x) (Applied Biosystems, ATF3, HS00231069), 10 µl of TaqMan Universal PCR Master Mix (2x) (Applied Biosystems, 4304437) and 7 µl of RNase-free water. The endogenous control for the assay was the housekeeping gene, human GAPDH (20x) (Applied Biosystems, HS4333764-F).

The reaction was performed in a 7500 Real-Time PCR system (Applied Biosystems). Other TaqMan Primers/Probes (ATF4: HS00909569_G1; DDIT4: HS01111686_G1; HMGCS1: HS00940429_M1; INSIG1: HS01650977_G1; HMGCR: HS00168352_M1; DDIT3: HS00358796_G1; RHOA: HS00357608_M1; BNIP3: HS00969291_M1)

2.6 Propidium Iodide Flow Cytometry

One million SCC25 and SCC9 cells were seeded in 10 cm plates and incubated overnight to allow for attachment and recovery. The next day the cells were pretreated with 0, 1 or 5 µM monensin or 10 µM lovastatin and then incubated overnight. Twenty four hours later cells where treated with 1 or 10 µM erlotinib alone or in combination with monensin or lovastatin and incubated overnight. On the following day the media from the plates were collected in 50 ml Falcon tubes and washed with 10 ml PBS which was also added to the same 50 ml tubes containing the media. Two ml of trypsin was added to each plate. When cells were trypsinized, 10 ml of media was added to the plate, triturated and added to the corresponding 50 mL tube. Cells were then centrifuged at 1500 RPM for 5 minutes at 4 C, the supernatant was aspirated and the pellet was washed by resuspending in 10 ml of cold PBS and the cells were centrifuged again at 1500 RPM for 5 minutes at 4 C. Then the wash was aspirated and the cells were fixed in 3 ml of cold 80% ethanol overnight at -20 C. Cells were centrifuged again as before and the supernatant aspirated, pellet washed with 10 ml cold PBS, centrifuged, the wash aspirated and the pellet resuspended in 3 ml of staining buffer (0.2% Triton X-100 and 1 mM EDTA pH8 in PBS pH7.4) and incubated on ice for 5 minutes. Cells were centrifuged as mentioned previously, the supernatant aspirated and the pellet was resuspended in staining buffer containing 25 ug/ml propidium iodide (Sigma-Aldrich) and 40 ug/ml RNase A (BioShop, Burlington, Ontario, Canada) and incubated for a

minimum of 1 hour in the dark at room temperature. Data (10000 events) was acquired on an EPICS XL flow cytometer (Beckman Coulter, Brea, California, USA) and analyzed with Modfit software (Verity Software House, Topsham, ME, USA).

2.7 Trypan Blue Exclusion assay

SCC9, SCC25 and WI38 cell lines where seeded on 6-well plates at 3 x 10^5, 2.5 x 10^5 and 3 x 10^5 cells/well, respectively, and were incubated at 37ºC overnight for attachment. On the following day, cells were pretreated with 1 or 5 µM monensin for 24 hours. On the next day the cells were treated with 1 or 10 µM erlotinib alone or in combination with 1 or 5 µM monensin for another 24 or 48 hours for a total treatment time of 48 or 72 hours. After the treatment time had elapsed, the media were aspirated and the cells were washed with 3 ml of PBS. The PBS was aspirated and 200 µl of trypsin (Cellgro, Manassas, VA, USA) was added to each well and the cells were incubated at 37ºC to allow cells to detach. Eight hundred µl of complete media were then added to each well and the cells were triturated by gentle pipetting. The cell suspension was then transferred into a sample cup and cell count was performed using a Vi-Cell XR cell viability analyzer (Beckman Coulter, Brea, CA, USA).

2.8 Ex-Vivo Samples Processing, RNA Extraction and PCR

Samples were obtained from surgery and were kept in complete media until processing time. A biopsy punch was used to cut sample cores that are about 2 mm in diameter. Each 2 mm core was further cut to two or three smaller pieces using a razor blade to increase surface area exposure to drug; the pieces were then randomized and distributed onto a 24-well plate. Each treatment was done in triplicates of control, 1, 10, or 25 µM of

monensin. Each well contained four pieces and treatment was done for 48 hours. Cores were transferred into 1.5 ml screw-cap tubes without the media and snap frozen in liquid nitrogen. At the time of RNA isolation, the samples weights ranged from 29 to 36 mg. Trizol (Invitrogen, Carlsbad, CA, USA) RNA isolation protocol, as described by Chomczynski et al. (105), was followed to extract total RNA from the tissue. Briefly, 0.5 ml of trizol was added to each tube and homogized using PowerGen 125 tissue homogenizer (Fisher Scientific, Hampton, NH, USA) until there were no visible tissue pieces and incubated at room temperature for about 5 minutes to allow full dissociation of nucleoprotein complexes. 100 µl of chloroform were added to each sample and then vortexed for 15 seconds and incubated further at room temperature for another 5 minutes. The samples were then centrifuged at 12000 g for 15 minutes at 4 °C. The aqueous phase was then transferred to a new Eppendorf tube and the RNA was precipitated by adding 250 µl of isopropanol and incubated at room temperature for 10 minutes and then centrifuged at 12000 g for 10 minutes at 4 °C. Following centrifugation the pelleted RNA was washed with 1 ml of 75 % ethanol and then centrifuged at 7500 g for 5 minutes. The ethanol wash was then aspirated and the pellet was washed a second time with 0.5 m of 75% ethanol. Samples were again centrifuged at 7500 g for 5 minutes, the ethanol was aspirated and the samples were left to dry for 5 minutes before dissolving in 30 µl of water. RNA concentration was measured using a Take3 Micro-Volume plate and BioTek Synergy MX plate reader and analyzed using Gen5 software (BioTek, Winooski, VT). Reverse-transcription was performed as has been mentioned earlier for cell lines with the difference that 0.7 µg of RNA was used since we were limited by the RNA quantity extracted from tissue. RT-PCR was also performed as previously described for the cell lines.

2.9 Fluorescence Microscopy

SCC25 cells were seeded in 6-well plates containing a cover slip at a density of 2.5 x 10^5 cells/well in complete media and incubated overnight at 37 °C and 5% CO_2 to attach. The next day, complete media were replaced by serum free media and cells were treated with control, 0.1, 1, 10 µM erlotinib, 10 µM lovastatin, and 1 µM monensin for 24 hours. A modification from a flow cytometry procedure by Wang et al. (106) was followed from here on. The following day the cells were treated with 100 ng/ml EGF that is conjugated to the Alexa-488 flourophore (Molecular probes, Eugene, Oregon, USA) for 30 minutes at 4 °C to allow the ligand to bind to the receptor but not internalize. After that the cells were washed three times with 2 ml ice-cold PBS followed by 15 minutes incubation at 37 °C to allow for internalization. Then, cells were incubated on ice to stop internalization, rinsed three times with ice-cold PBS and then acid washed for 5 minutes with 2 ml of acetic acid solution (0.2 M acetic acid and 0.5 M NaCl, pH 2.8). This step ensures that any ligand bound to receptor that is still on the cell surface will be washed away and thus only ligands that have already internalized into the cells are shielded from the wash. Following that, the cells were washed three times with PBS and fixed with 2 ml solution of 4% paraformaldehyde (Sigma-Aldrich) (4% w/v paraformaldehyde, 2 mM $MgCl_2$, 1.25 mM EDTA in PBS, pH 7.3) for 15 minutes at 37 °C. Cells were then washed two times with PBS and mounted on a microscope slide with VectaShield mounting media with DAPI (Vector Laboratories, Burlingame, CA, USA). The slides were sealed with nail polish and incubated in the dark for 5 minutes to dry, and then examined under a Ziess inverted microscope (Ziess, Oberkochen, Germany) using oil immersion microscopy.

A similar procedure was followed for the LDL internalization. SCC25 were seeded on 6-well plates as mentioned previously and incubated overnight for attachment. The next

day the cells were treated with 0, 1 or 5 µM monensin for 48 hours. 1 ug/mL LDL-Alexa 488 (Molecular Probes) was added to the media and cells were incubated for 15 minutes at 37ºC to allow the LDL to internalize. Following stimulation with LDL, the cells were washed three times with PBS and then fixed with 4% paraformaldehyde for 15 minutes at 37 °C. The cells were then washed two times with PBS and mounted on microscope slides using VectaShield mounting media with DAPI (Vector Laboratories) and sealed with nail polish, dried, and examined using the Ziess inverted microscope (Ziess).

3.0 Statistical Analysis

MTT data are expressed as the mean of six replicates, all other experiments were done in triplicates. Error bars are the SD from the mean. Statistical differences were determined by analysis of variance (ANOVA) test and $p<0.05$ was considered to be statistically significant.

Chapter 3: Results

3.1 Monensin Synergistically Enhances the Cytotoxicity of Lovastatin and Erlotinib

After analyzing the high throughput screen results it was essential to validate the effect of monensin on the cytotoxic effect of lovastatin and erlotinib. A series of MTT cell viability assays were designed for that purpose. The assay contains three controls to which the cell viability was compared: the first is a negative control where there are no cells in the wells and this corresponds to 0% viability, the second control is the positive control which contains untreated cells and thus corresponds to 100% viability, and finally the solvent control contained cells treated with ethanol (the solvent for lovastatin and monensin) and DMSO (the solvent for erlotinib) the viability of which was always greater than 90% (not presented). Synergism is defined and calculated as described by Chou and Talalay (107). Briefly, CI values of <1, >1 and equal to 1 represent synergism, antagonism and additive

effect, respectively. In HNSCC cell lines, SCC9 and SCC25, monensin combination with lovastatin resulted in a marked decrease in viability in a dose dependent manner (Figure 3.1) which was also found to be a synergistic effect when analyzed on a Fa-CI plot (Figure 3.3 top panels).

The difference, between the group of cells treated with monensin as a single agent and the group of cells treated with monensin and lovastatin, was statistically significant as calculated by the two-way ANOVA test ($p<0.0001$). Furthermore, monensin's effect on the cytotoxcity of erlotinib was confirmed also in a dose dependent manner (Figure 3.2) and was also synergistic (Figure 3.3 bottom panels). In both cases of combination of monensin with either lovastatin or erlotinib, the SCC9 cell line appeared to be more sensitive to treatment.

As mentioned, previous work in our laboratory showed that lovastatin in combination with erlotinib leads to a more potent, synergistic cytotoxic effect using MTT assay; therefore, we attempted to study the effect of the addition of monensin in a triple combination treatment with lovastatin and erlotinib on the viability of the SCC cell lines. Figure 3.4 shows that, in SCC9, the addition of 0.1µM monensin in combination with the other drugs leads to high cytotoxicity and eradicates the cells leaving about 10% or less viable cells. On the other hand, the addition of 0.1µM monensin to the combination of lovastatin (1 and 5 µM) with erlotinib in SCC25 showed a dose dependent increase in cytotoxicity.

Next, we evaluated the effect of monensin on a SCC9 clone that is highly resistant to lovastatin and assess whether the addition of monensin would sensitize the cells to lovastatin. In figure 3.5 we compared the effect of the drugs in question on the viability of the SCC9 R4 clone using MTT assay.

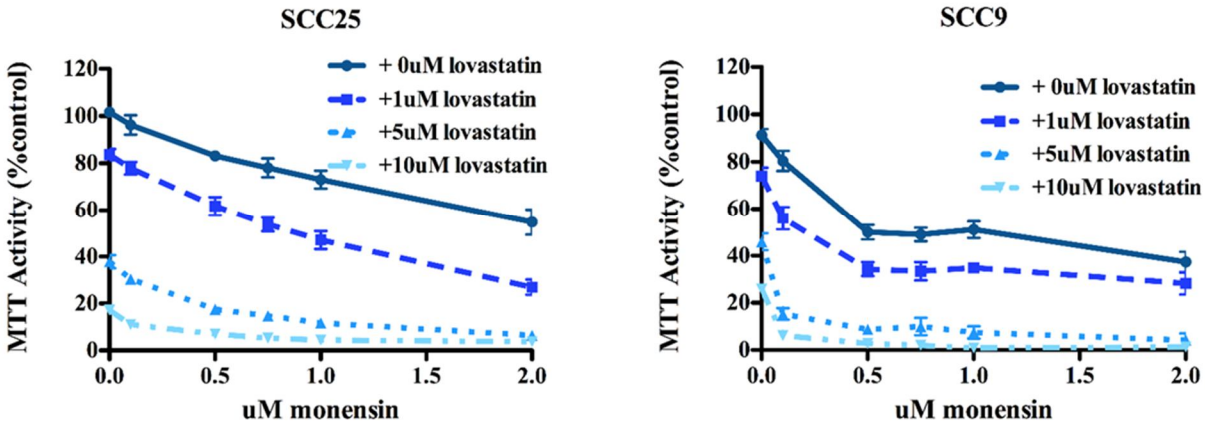

Figure 3.1. MTT Cell Viability Assay (lovastatin + monensin combination treatment). Lovastatin pretreated cells for 24 combined with increasing concentration of monensin for 48hours for a total treatment of 72 hours. Line graphs showing the MTT activity presented as % of control as a function of concentration of monensin. Combining lovastatin with monensin leads to further decrease in cell viability. Data are presented as the average of six replicates and error bars are SD from the mean.

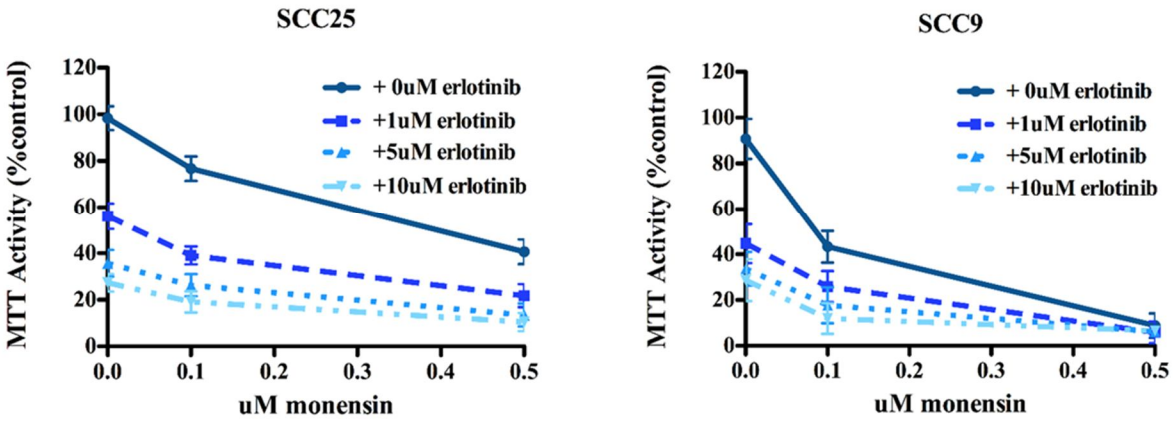

Figure 3.2. MTT Cell Viability Assay (monensin + erlotinib combination treatment).

Monensin pretreated cells for 24 combined with increasing concentration of erlotinib for 48hours for a total treatment of 72 hours. Line graphs showing the MTT activity presented as % of control as a function of concentration of monensin. Combination of monensin with tarceva leads to a dramatic decrease in cell viability. Data are presented as the average of six replicates and error bars are SD from the mean.

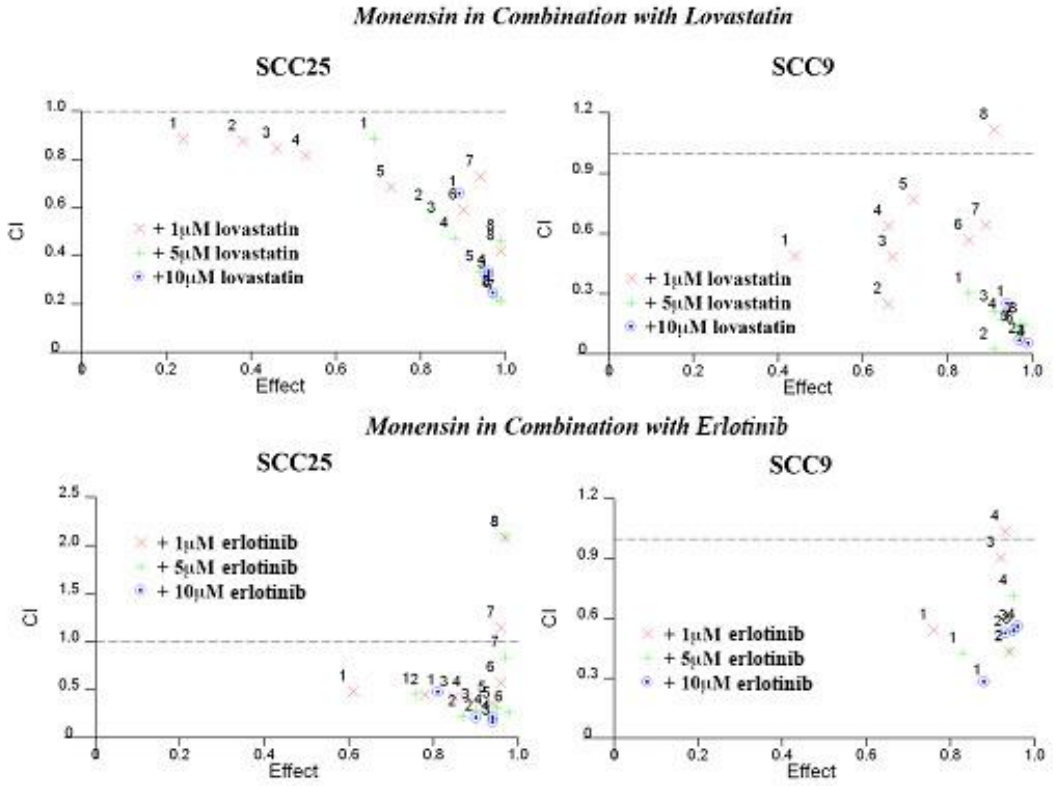

Figure 3.3. Fa-CI Plots for Drugs Combination. These plots show the synergistic effect of monensin in combination with lovastatin (top row of panels) or erlotinib (bottom row of panels). Combination indices (CI) below one are considered synergistic, CI above one are considered antagonistic, and CI at or close to one are considered additive as described by Chou and Talalay.

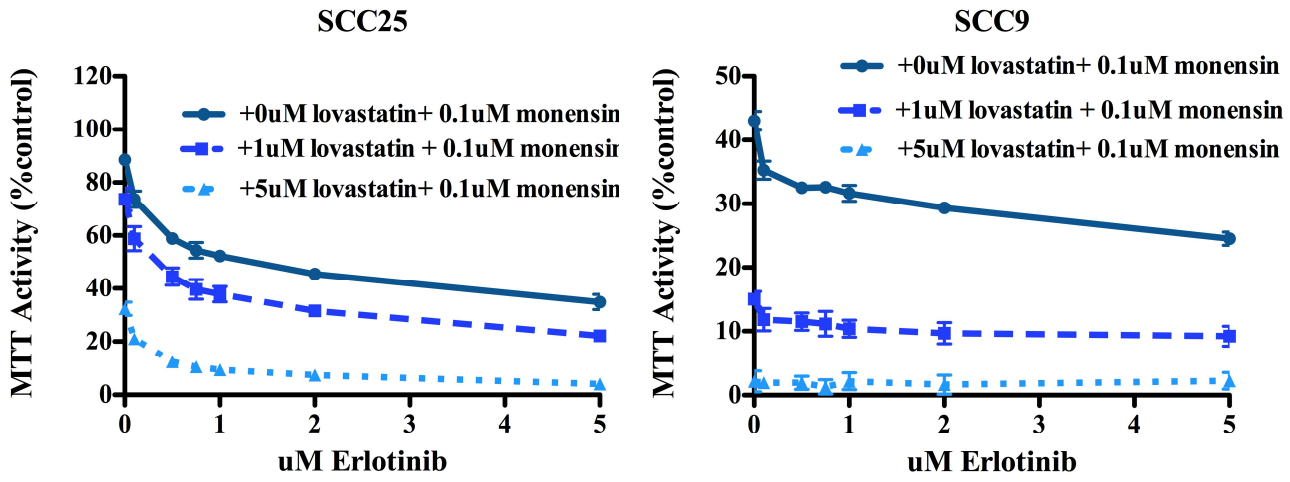

Figure 3.4. MTT Cell Viability Assay (Triple Drug Combination Treatment).
0.1 µM monensin + 1 or 5 µM lovastatin pretreated cells for 24 combined with increasing concentration of erlotinib for 48 hours for a total treatment of 72 hours. Line graphs showing the MTT activity presented as % of control as a function of concentration of erlotinib. Triple combination treatment leads to a more dramatic cytotoxic effect even at lower concentrations. Data points presented are the mean of six replicates and the error bar is the SD.

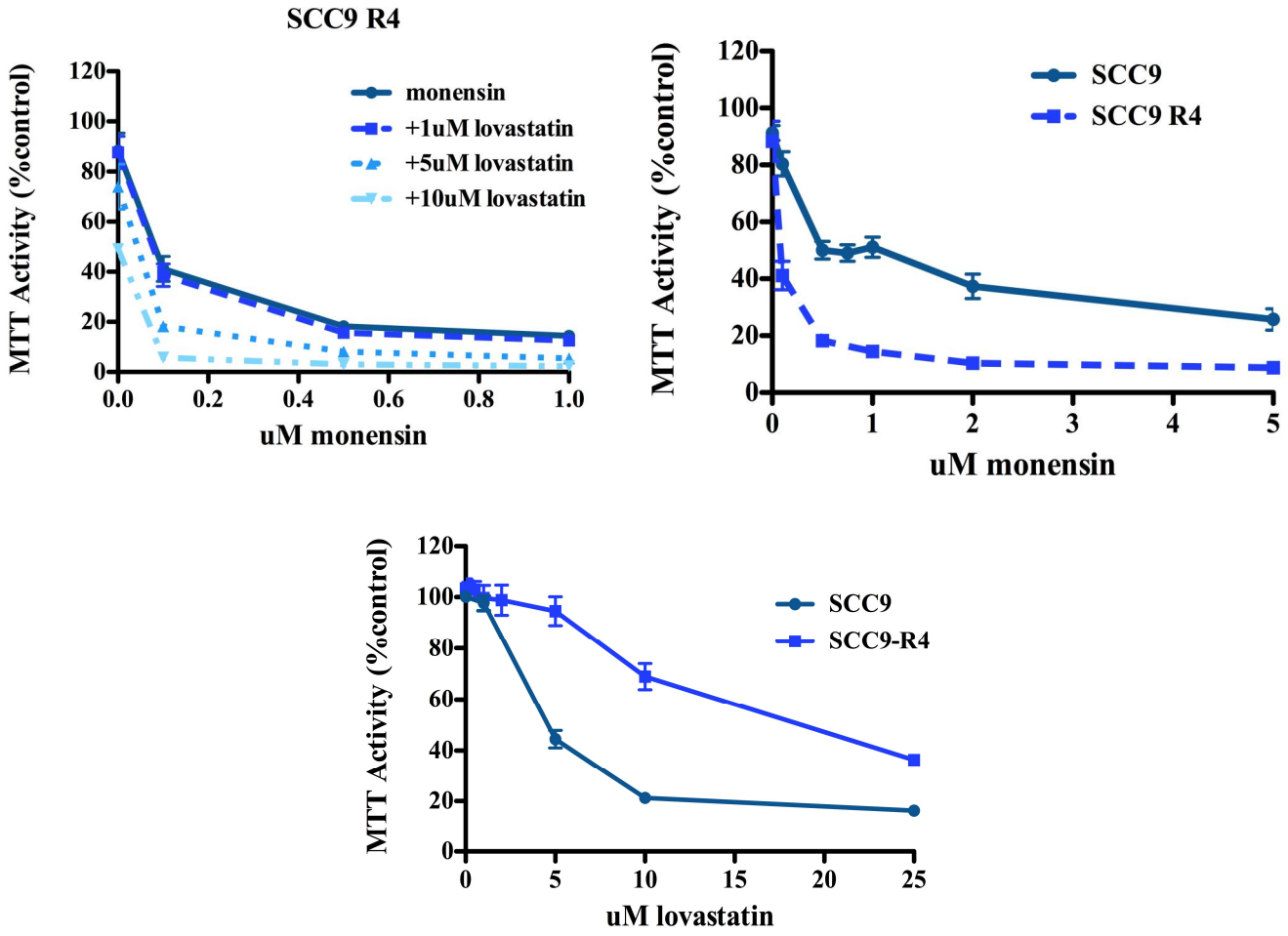

Figure 3.5. MTT Cell Viability Assay; lovastatin Resistant SCC9. The effect of monensin on the lovastatin resistant subclone of the SCC9 cell line alone and in combination with lovastatin (upper left panel). Comparison of the sensitivity to monensin between the lovastatin resistant clone and the parental cell line shows that SCC9 R4 is more sensitive to monensin treatment (upper right panel). The Lower panel shows that the SCC9 R4 is more resistant to lovastatin than the parental cell line.

Treatment with lovastatin for 48 hours did not affect the viability of the clone significantly (viability around 95% at 5µM lovastatin for 48 hours; data not shown). However, the addition of only 1µM monensin for 48 hrs shows a dramatic decrease of cell viability (below 20%). Furthermore, pre-treatment with 1, 5, or 10 µM lovastatin lead to further enhancement of cytotoxicity. Comparison of sensitivity to monensin between the resistant SCC9-R4 and the parental SCC9 cell lines showed a significant difference (Figure 3.5 right panel) with the resistant cell line being more sensitive to monensin.

We endeavoured to confirm the effect of monensin on the SCC cell lines using a different method. By performing Trypan blue exclusion assay we evaluated the effect of 48 and 72 hours treatment of monensin and erlotinib and compared the cell counts of SCC9 and 25 with those of the normal human fibroblast cell line WI-38. As seen in figure 3.6 the cell counts in the SCC9 cell line fall to about 20 % or less when monensin is combined with erlotinib, while the cell counts vary between 40 and 20% in the case of the SCC25 cell line (Data not shown). However, the cell counts in the WI-38 cell line remained above 75%. After 72 hours of treatment, on the other hand, the cell counts in the SCC cell lines fall below 10% in the combination treatment while in the WI-38 normal fibroblasts the cell counts were higher than 30% (data not shown).

3.2 Monensin Induces a Potent Apoptotic Response in Combination with Erlotinib

To further confirm the ability of monensin to potentiate the cytotoxicity of erlotinib, we performed propidium iodide flow cytometric analysis to look at apoptotic response. SCC25 and SCC9 cells were pretreated with 1 or 5 µM monensin, or 10 µM lovastatin for 24 hours, followed by 24 hours treatment with 10 µM erlotinib alone or in combination with the other drugs for a total treatment of 48 hours; each condition was done in triplicates.

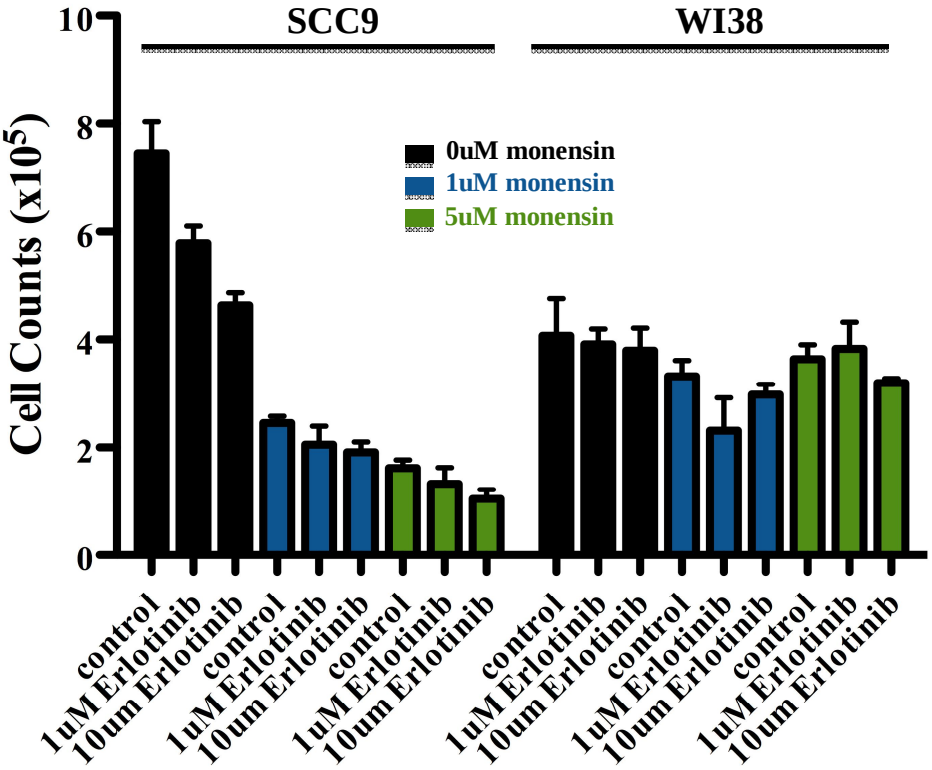

Figure 3.6 Trypan Blue Exclusion Assay. Comparison of the counts of viable cells of two cell lines (SCC9 and WI-38) after 48 hours of the indicated treatments. Pretreatment of SCC9 with monensin for 24 hours greatly reduced viable cells, on the other hand the normal fibroblast cell line, WI38 were not affected to the same degree. Black represents cells not treated with erlotinib only, blue represents cells pretreated with 1uM monensin for 24 hours followed by 24 hours combination with erlotinib, green represents cells pretreated with 5 uM monensin for 24 hours followed by 24 hours treatment with erlotinib. The error bars represent SD from the mean of three replicates (n=3).

Figure 3.7 shows the histograms of the different treatment conditions and the number shown represents the percentage of apoptosis. Untreated cells showed around 2.5% apoptosis; on the other hand, 48 hours treatment with 1µM monensin resulted in a slight increase in apoptosis (4.5%). Treatment with 5 µM monensin for 48 hours had a greater effect on apoptosis (16.4%). 10 µM lovastatin for 48 hours had a higher apoptotic response than 1µM monensin, but lower than 5 µM monensin (4.5% 1µM monensin< 9.6% 10 µM lovastatin<16.4% 5 µM monensin). Erlotinib treatment for 24 hours at 10 µM resulted only in a slight increase of apoptosis when compared to control (3.4%). Pretreatment with 1µM monensin for 24 hours followed by 10 µM erlotinib treatment for another 24 hours resulted in a marked increase in apoptotic events (14.6%) when compared to 1µM monensin alone. Additionally, combination of 5µM monensin with 10 µM erlotinib showed the highest percentage of apoptosis (38.7%). Combination of lovastatin with erlotinib on the other hand resulted in a modest increase in apoptosis when compared to lovastatin alone (13.2% and 9.6% respectively). The SCC9, on the other hand, apoptosis induction did not show a similar pattern to SCC25 under the same conditions of treatment (Figure 3.8). Under control conditions 3.5% of the population were in the sub G1 component; treatment with 1µM monensin or 10 µM erlotinib only increased apoptosis to about 7% while treatment with 5 µM monensin alone or in combination with 10 µM erlotinib, and 10 µM lovastatin alone or with 10 µM erlotinib induced apoptosis to about 23%. The results are quantified for a side by side comparison in figure 3.9. Collectively with the cell counts and MTT assays, these results show that monensin is a potent inducer of apoptosis and synergistically enhances the cytotoxic effects of both lovastatin and erlotinib in combination. The histograms also show notable variations in the G1 and S phases with the different treatments which might indicate that the drugs affect the cell cycle; however, this will require further investigation.

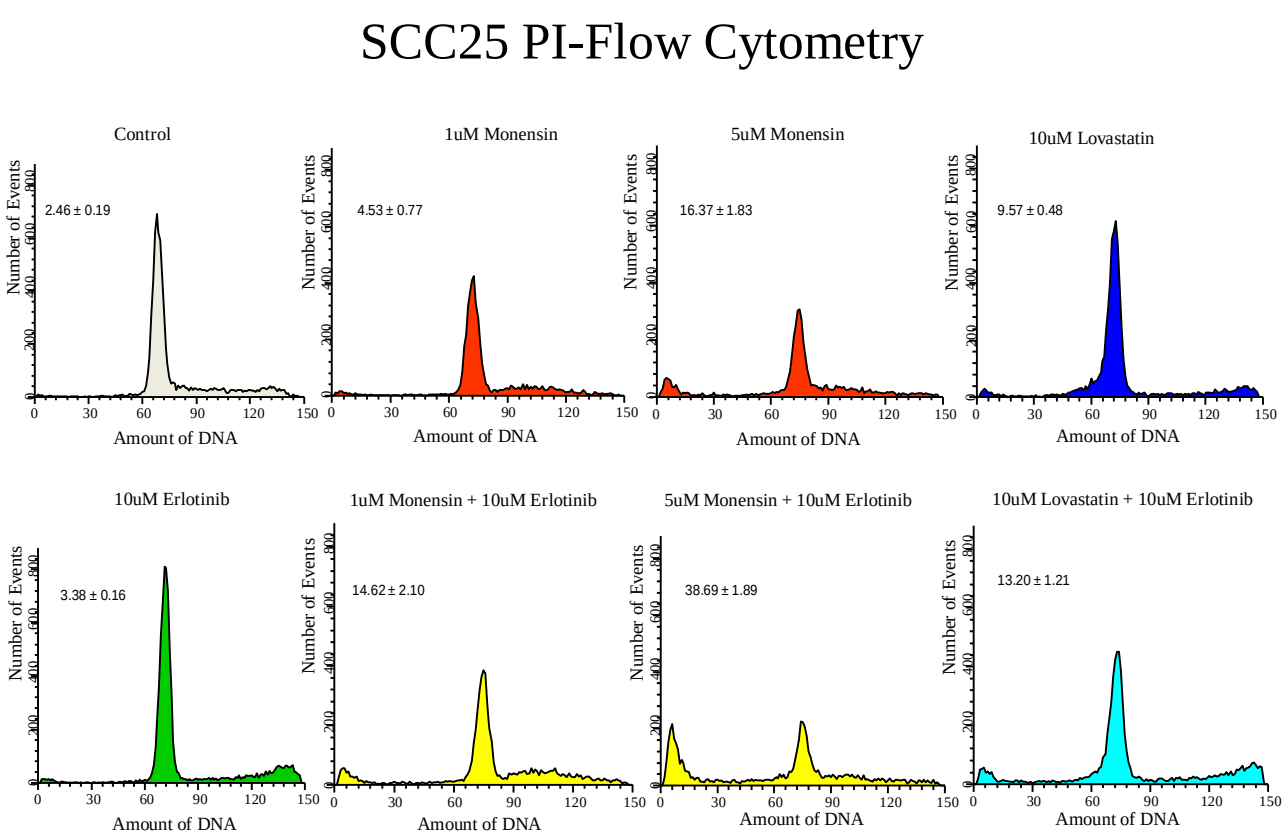

Figure 3.7. SCC25 Propidium Iodide Flow Cytometry. Histograms of flow cytometry data showing, in the top row of panels from left to right, control, 1 µM monensin, 5 µM monensin and 10 µM lovastatin. The bottom row of panels 10 µM erlotinib and its combination with the mentioned drugs. Combination of monensin with erlotinib dramatically increased apoptosis in SCC25 cells.

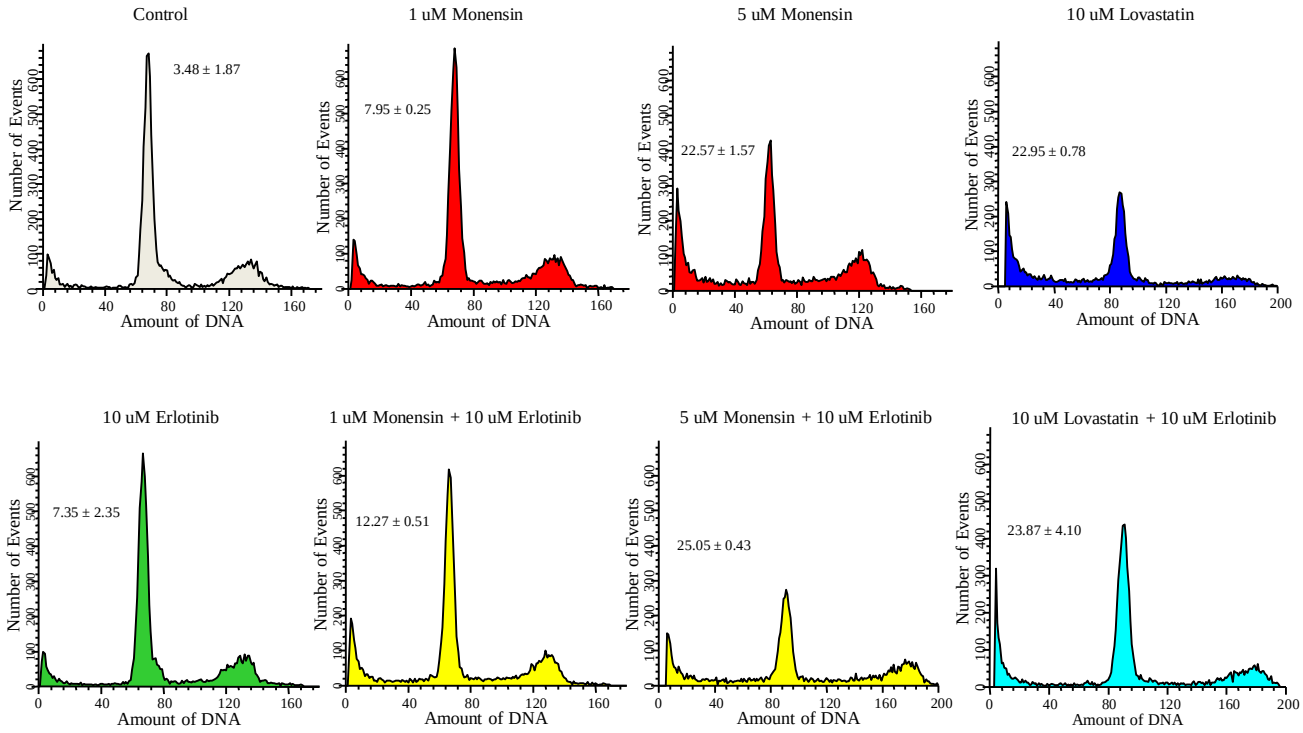

Figure 3.8. SCC9 Propidium Iodide Flow Cytometry. Histograms of flow cytometry data showing, in the top row of panels from left to right, control, 1 µM monensin, 5 µM monensin and 10 µM lovastatin. The bottom row of panels 10 µM erlotinib and its combination with the mentioned drugs. Monensin is capable of inducing an apoptotic response as potent as its combination with erlotinib in the SCC9 cell line.

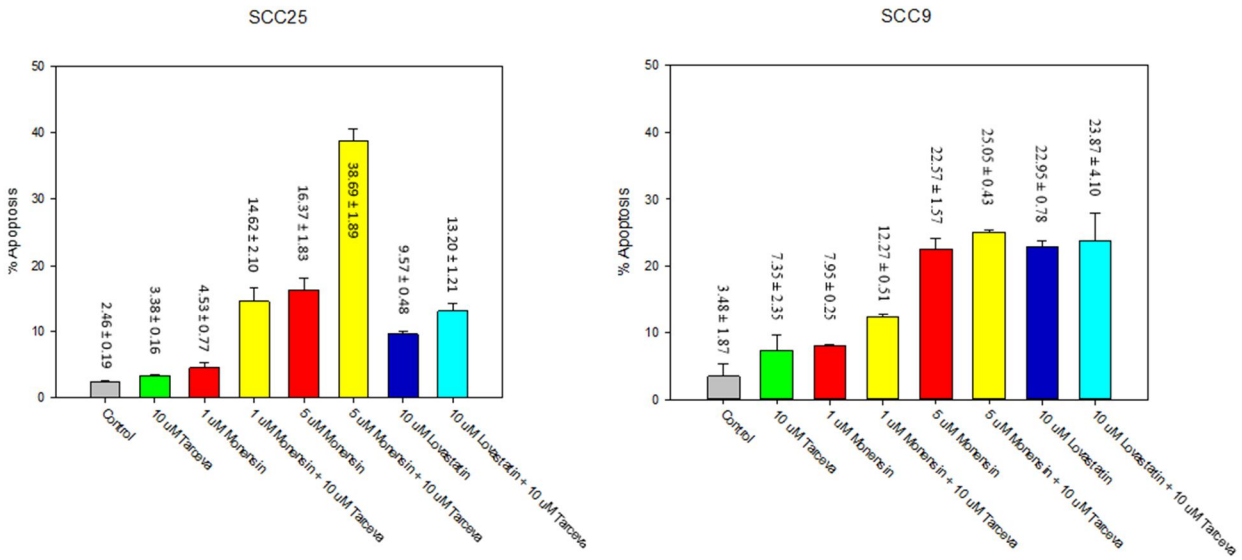

Figure 3.9. Flow Cytometry Qantification. A bar diagram that summarizes the data from the flow cytometry experiments by plotting the % of Apoptosis as a function of treatment. The colours correspond to the histogram of the respective treatment. Combination of monensin and erlotinib can induce a potent apoptotic response. Error bars represent the SD from the mean; n=3.

3.3 Monensin Enhances the Phosphorylation Inhibition Capacity of Erlotinib

The effect of the combination of monensin with erlotinib was further assessed on EGFR cell signalling pathways using western blot and densitometric analysis. Phosphorylation status of EGFR, Akt and ERK proteins was assessed (Figure 3.10 upper panels). For pEGFR, monensin enhanced the ability of erlotinib to inhibit phosphorylation of the receptor. This is supported by densitometric quantification shown in Figure 3.10 (lower panels). Erlotinib partially inhibited the phosphorylation of Akt at 10 and 1 µM but had no effect at lower concentrations as compared to the control; addition of monensin had no effect on the phosphorylation of Akt. On the other hand, while erlotinib inhibited phosphorylation of ERK1/2 at 10 and 1 µM concentrations, monensin resulted in the reactivation of ERK1 but not ERK2.

3.4 Erlotinib, Lovastatin and Monensin Interfere with the EGFR Trafficking

Previous studies have demonstrated that monensin is a robust inhibitor of intracellular trafficking including the ability to inhibit trafficking of the EGFR (108, 109). In an attempt to assess the effect of the drugs that are evaluated in this study on the trafficking of the EGFR we utilized an Alexa-488 tagged EGF ligand and followed its localization with fluorescent microscopy. SCC25 cells were treated with control, 10, 1 and 0.1 µM erlotinib, 10 µM lovastatin, or 10 µM monensin for 24 hours in serum free media and then stimulated with the tagged ligand. As shown in figure 3.11, after 15 minutes at 37 °C, untreated cells display a uniform punctuate distribution pattern of green fluorescence, which corresponds to the ligand-receptor complex, throughout the cell. Addition of 10 µM erlotinib to the culture, however, resulted in absence of fluorescence.

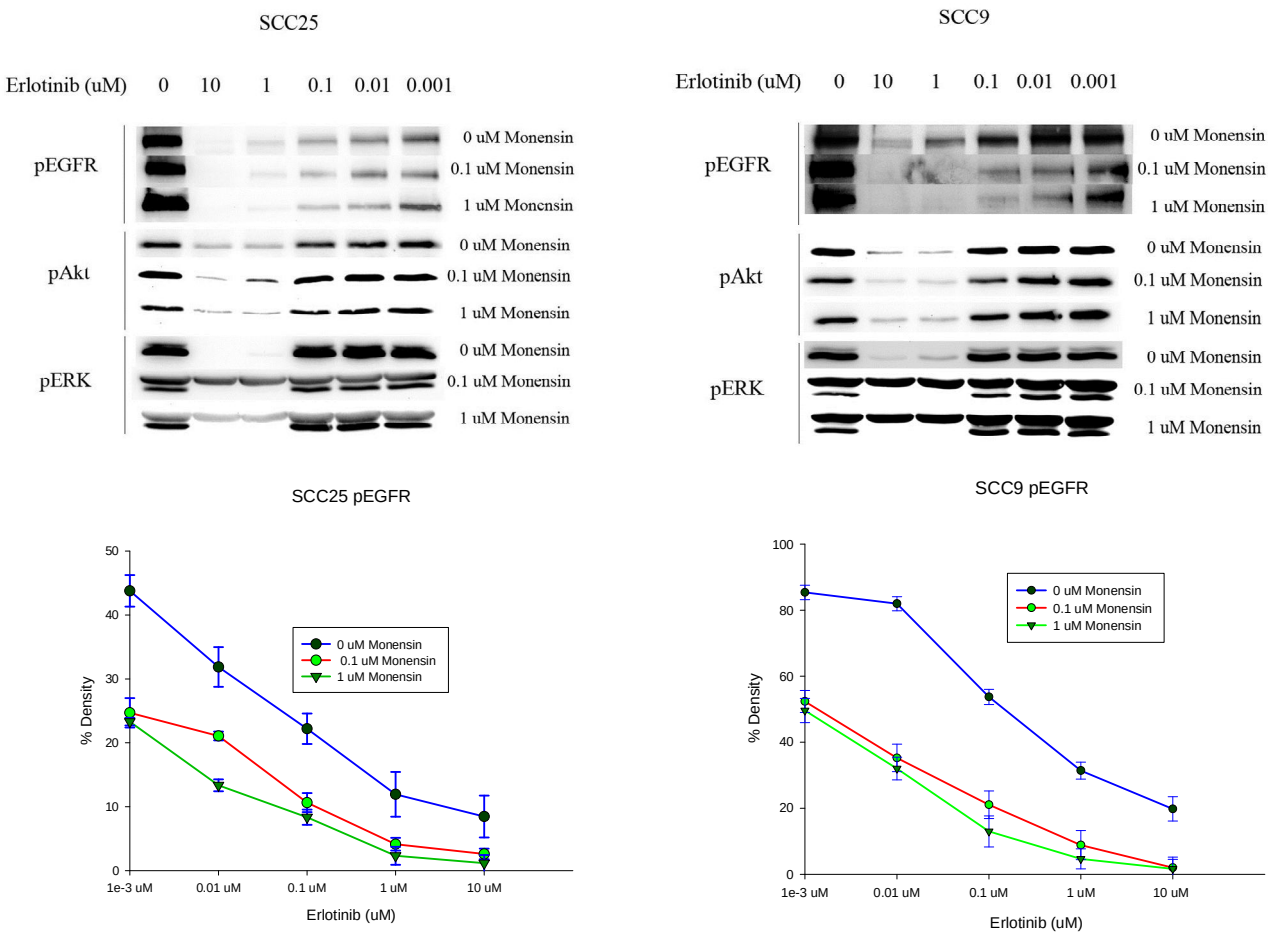

Figure 3.10. Wester Blot and Densitometric Analysis of Erlotinib and Monensin Treated Cells. Top panels show the Western blots of phospho-EGFR, -Akt, and -ERK in monensin and erlotinib treated cells followed by EGF stimulation. Bottom panels show the densitometric analysis of the pEGFR. Monensin pretreatment enhanced erlotinib's ability to inhibit phosphorylation of the EGFR; however, Akt and ERK phosphorylation was not affected. The error bars represent SD from the mean of three replicates (n=3).

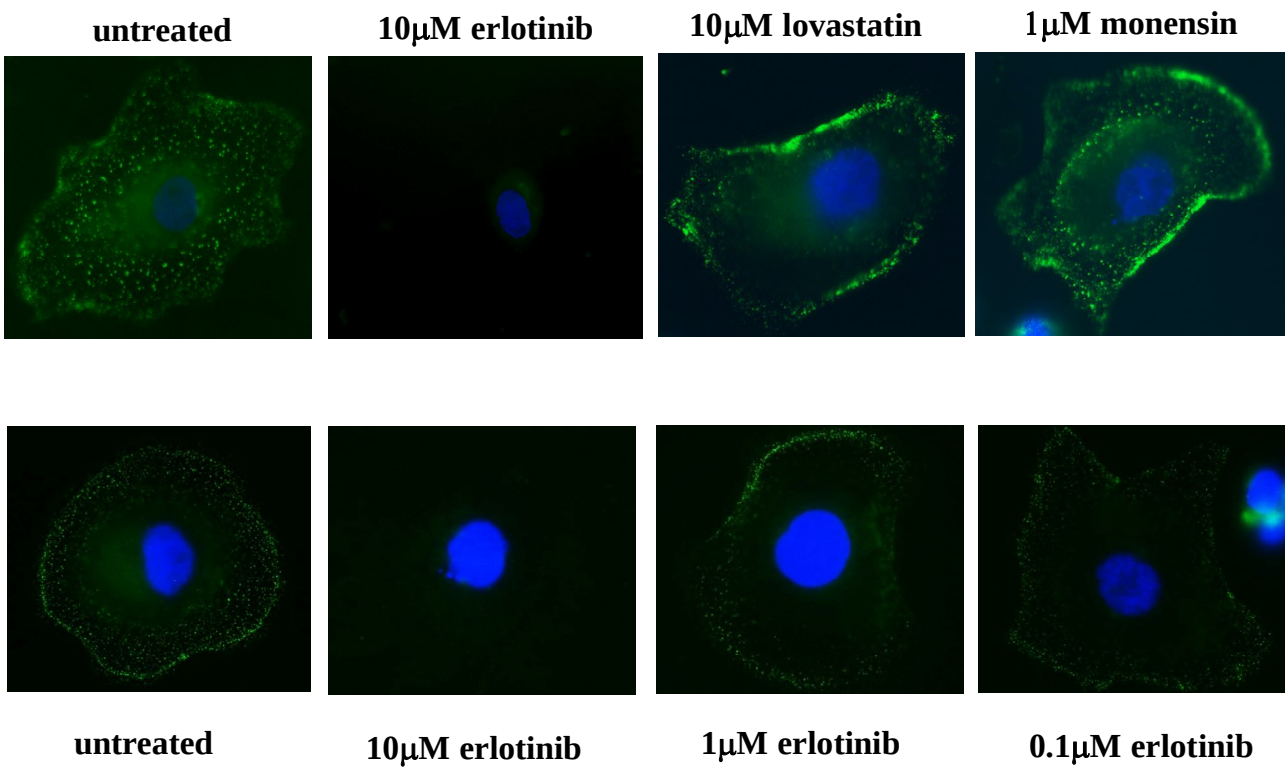

Figure 3.11. Effect of Treatment on EGF Internalization. The effect of 24 hours treatment of erlotinib (0.1, 1 and 10 uM), 10 μM lovastatin and 1 μM monensin on the ability of SCC25 cells to uptake the EGF ligand compared to untreated controls. Non-treated cells shows punctate bodies implying normal internalization of the ligand, treatment with 10 uM erlotinib inhibited internalization of the ligand. On the other hand, treatment with 10 um lovastatin or 1 uM monensin lead to accumulation of the ligand close to the cytoplasmic membrane indicating impaired trafficking. As a control, SCC25 cells were treated with decreasing concentrations of erlotinib and we show as the concentration of erlotinib decreases cells restore their ability to take up the ligand. Green represents Alexa-488 tagged EGF and blue represents DAPI stain.

On the other hand, treatment with 10 µM lovastatin or 1 µM monensin lead to accumulation of the fluorophore near the cytoplasmic membrane indicating a failure to traffic the ligand/receptor complex within the cell. To confirm the effect of erlotinib on the uptake of the ligand, we treated cells with a logarithmically decreasing concentration of the drug and added the ligand. As can been seen in the figure, the drug inhibits the internalization of the ligand at 10 µM concentration but had little effect at 1 and 0.1 µM. These results show that all three drugs have the ability to interfere with the normal trafficking of the EGF receptor albeit through different mechanisms.

3.5 Monensin Activates Pathways Implicated in Lipid Synthesis and Apoptosis

In order to gain an insight on the effect of monensin on the transcriptome of an in-vitro cell model, we treated SCC25 cells with control or 1 µM monensin for 24 hours followed by total RNA extraction. The RNA was sent to StemCore (Ottawa, ON, CA) in the OHRI and RNA-Seq analysis was performed. To narrow the list of hits we selected some of the genes in which the difference in expression between the control and the treated sample was at least four times, which reduced the number of hits to just over 150 targets. Among these targets there were a few non-coding transcripts that were disregarded in this study. Interestingly, searching among the remainder of the targets we found a significant number of genes that are involved in lipid and cholesterol synthesis (Table 3.1 green highlight) and a few in other pathways like apoptosis and energy metabolism. To validate some of those hits we performed RT-PCR on SCC25 and SCC9 using primers for ATF3, ATF4, CHOP (DDIT3), HMG-CoA Reductase, Rab5, BNIP3, INSIG1, DDIT4, and HMG-CoA synthase1. The response to treatment was different in both cell lines although they both are tongue-derived squamous cell carcinoma cells (Figure 3.12).

Gene	Log2 Fold Change	Description
FADS2	3.52016	Desaturase enzymes cause desaturation of fatty acids
LPIN1	2.86845	Catalyzes the penultimate step in triglyceride synthesis
MSMO1	2.86593	Believed to function in cholesterol biosynthesis
HMGCS1	2.86524	3-hydroxy-3-methylglutaryl-CoA synthase 1
VLDLR	2.67433	Very-low-density-lipoprotein receptor
SQLE	2.52564	Squalene epoxidase catalyzes the first oxygenation step in sterol biosynthesis
ACSS2	2.51426	Catalyzes the activation of acetate for use in lipid synthesis and energy generation
INSIG1	2.48191	Important role in the SREBP-mediated regulation of cholesterol biosynthesis
PCSK9	2.34119	Plays a major regulatory role in cholesterol homeostasis, and induces LDLR degradation
HSD17B7	2.27139	17-beta-hydroxysteroid dehydrogenase 7
DHCR7	2.26534	7-dehydrocholesterol reductase
CYP51A1	2.26177	Synthesis of cholesterol by catalyzing there removal of the 14alpha-methyl group from lanosterol
STARD4	2.08509	StAR-related lipid transfer protein 4 (STARD4) is a soluble protein involved in cholesterol transport
FDFT1	2.0812	Farnesyl-diphosphate farnesyltransferase 1
SCDP1	2.0171	Stearoyl-CoA desaturase (delta-9-desaturase) pseudogene 1
IDI1	2.01286	Isopentenyl-diphosphate delta isomerase 1
HMGCR	2.01211	HMG-CoA reductase
MVD	2.0086	Mevalonate (diphospho) decarboxylase
FGF19	2.30896	Member of the fibroblast growth factor (FGF) family
TP53INP1	2.09804	p53-inducible nuclear protein 1
DDIT4	2.45967	Inhibits cell growth by regulating the TOR signalling pathway upstream of the TSC1-TSC2
CASP14	2.45942	Processed and activated by caspase 8 and caspase 10
NDUFA4L2	3.67361	NADH dehydrogenase (ubiquinone) 1 alpha subcomplex

Table 3.1. A List of Targets from RNA-Seq Analysis Data. This table shows a list of 23 genes that were deregulated by 1 µM monensin treatment. Eighteen genes (green) are implicated in lipid and cholesterol synthesis.

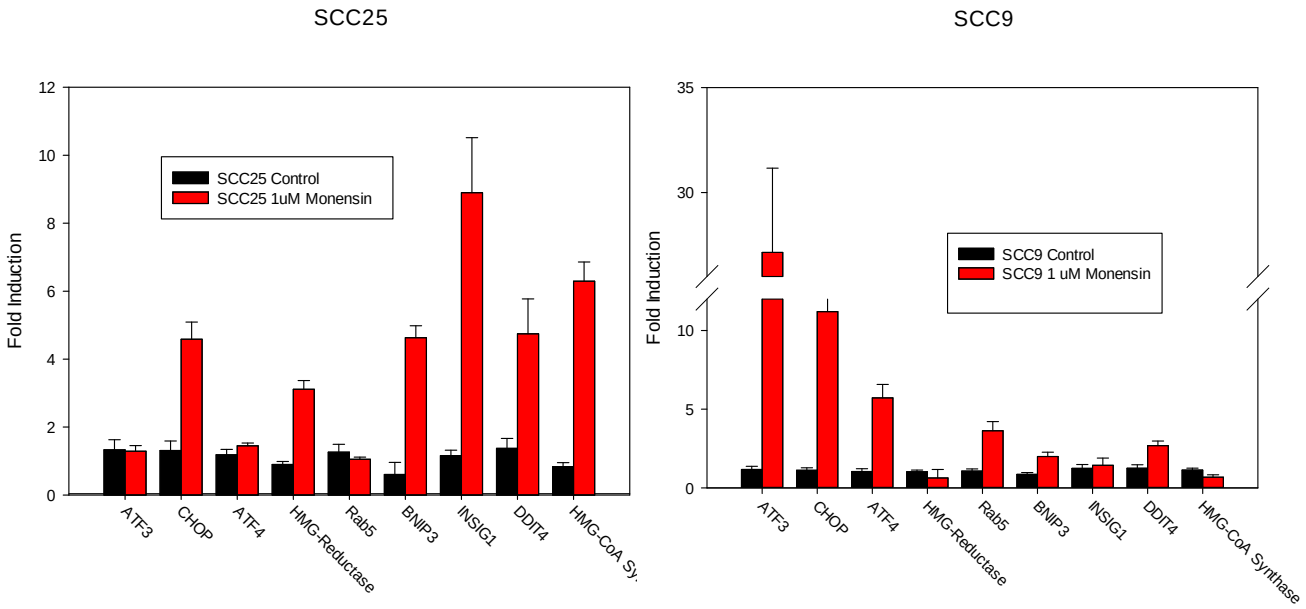

Figure 3.12. RT-PCR Analysis of Treatment with Monensin in Vitro. Comparison of the effect of 1 µM monensin treatment for 24 hours on the expression of ATF3, CHOP, ATF4, HMG-CoA reductase, Rab5, BNIP3, INSIG1, DDIT4, and HMG-CoA synthase genes between SCC9 and SCC25 cell lines. The RT-PCR results show that the two cell lines respond differently to treatment by upregulating different genes. In SCC25, genes that are involved in lipid metabolism as well as apoptosis regulating genes were upregulated, in contrast, stress response genes were upregulated in SCC9 cells.

In SCC9 ATF3, CHOP, and ATF4 were up-regulated dramatically (25, 10 and 5 times respectively) whereas Rab5 and DDIT4 were up-regulated around four and two times, respectively. In contrast, the majority of the genes that were up-regulated in SCC25 were not altered in the SCC9 cell line. In SCC25, INSIG1 was up-regulated about nine fold, HMG-CoA synthase was upregulated around six fold whereas CHOP, BNIP3 and DDIT4 were upregulated around four fold and lastly HMG-CoA Reductase was upregulated three fold (Figure 3.12).

3.6 Monensin Inhibits LDL Internalization

Two genes that were deregulated in the RNA-Seq data were the LDL-receptor (2.7 folds) and the PCSK9 gene (five fold) which are proteins associated with cholesterol uptake. The LDL receptor binds to Low Density Lipoproteins (LDL) that contain cholesterol and PCSK9 is a convertase that actively degrades the LDL receptor. In order to assess the effect of monensin on LDL uptake, SCC25 cells were treated with 0, 1µM and 5 µM monensin for 48 hours and then stimulated for 15 minutes with Alexa-488 tagged LDL at 37 °C. In Figure 3.13, we show that untreated cells readily took up the LDL, however, monensin inhibited the uptake of LDL partially, at 1µM concentration, and more completely at 5 µM concentration. This experiment shows that monensin inhibits the endocytosis of LDL in a dose dependent manner.

3.7 Treatment of Ex-Vivo Samples with Monensin Induces Activation of Apoptotic Markers

After evaluating the effect of monensin in vitro, we then moved to assess its potential by using ex-vivo samples from a variety of patients.

LDL Receptor Internalization

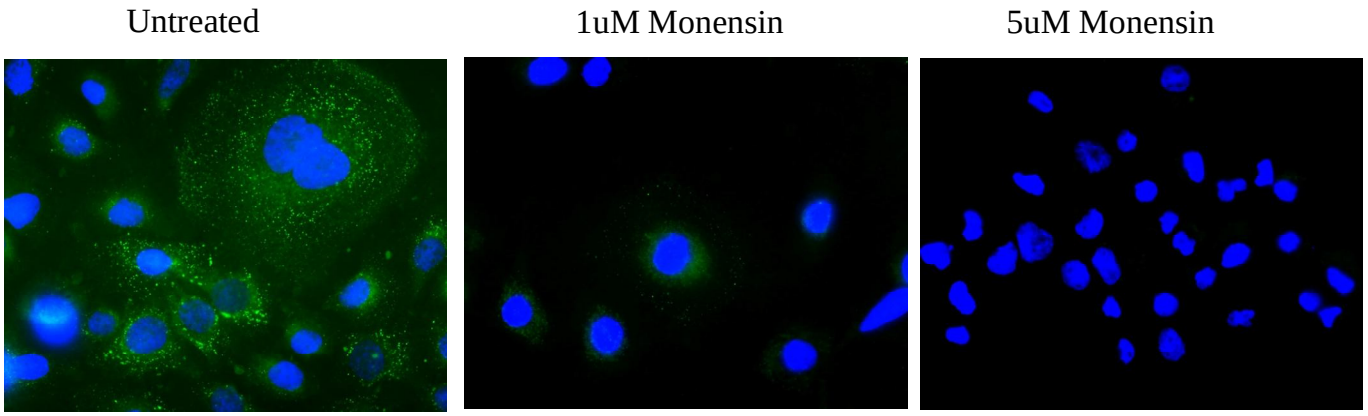

LDL-Alexa 488
DAPI

Figure 3.13. Effect of Monensin on the Internalizatoin of LDL. This figure shows the effect of 1 and 5 µM monensin treatment for 48 hours on the uptake of LDL in vitro using the SCC25 cell line. Untreated cells normally internalized LDL, whereas treatment with monensin inhibited its uptake. Green color represents Alexa-488 tagged LDL and blue is DAPI stain.

Six HNSCC, two ovarian cancer and two lung cancer patients' samples were treated with 0, 1 or 10 µM monensin for 48 hours followed by RT-PCR analysis of several target genes (Figures 3.14 and 3.15). Five out of the total ten samples, HN01; HN03; HN05; LU02 and OV01, showed significant induction of the apoptosis-regulating genes ATF3 and CHOP. On the other hand the other five samples showed a weak, or no induction of the studied genes. HN01 responded very well to the treatment; ATF3 was up-regulated five fold and CHOP was up-regulated around eight fold with 1 µM monensin treatment. Treatment with 10 µM monensin increased the induction of ATF3 to 30 fold compared to control, however, CHOP was induced about seven times the control. HN02 showed a very weak response to both 1 and 10 µM monensin treatment. Treating the samples from HN03 with 1 µM monensin did not induce ATF3 or CHOP significantly, however, 10 µM monensin resulted in about five and four times induction of ATF3 and CHOP, respectively. HN04 samples were not responsive to treatment although HMG-CoA reductase was upregulated about three times. Samples from HN05 responded slightly to 1µM monensin where all the genes involved were upregulated about two times the control, on the other hand, treatment with 10 µM monensin increased the induction to about five times for ATF3 and about three times for CHOP and HMG-CoA reducase. No significant difference was observed between treatment and control in HN06 samples. The lung sample taken from LU01 responded slightly to treatment with no apparent significant difference between 1 and 10 µM monensin treatment although CHOP was upregulated around two times. On the contrary, the samples taken from LU02 robustly responded to treatment; 1 µM monensin induced ATF3, CHOP, and HMG-CoA reductase two, four and three times, respectively, and 10 µM increased the induction to nine, eight and four times, respectively. Moreover, one of the two ovarian cancer samples, OV01, responded more readily to treatment.

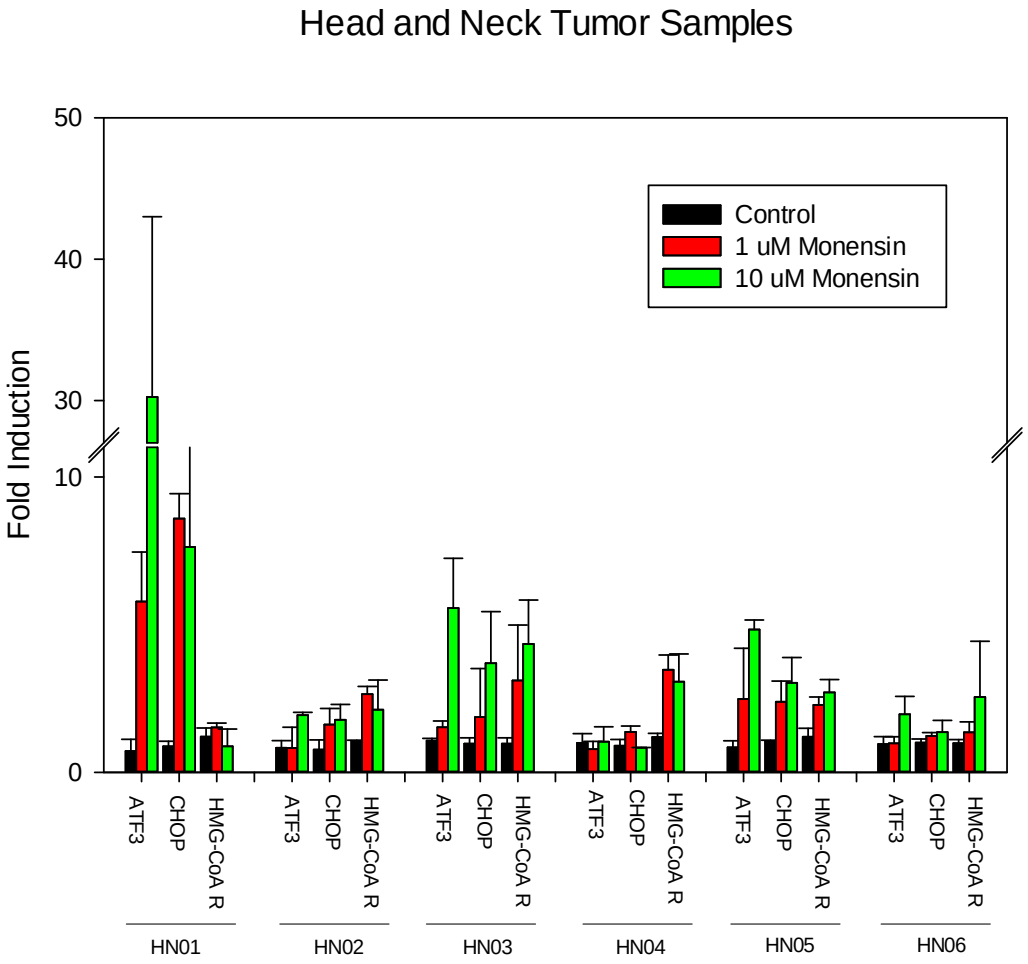

Figure 3.14. RT-PCR Analysis Performed on Head and Neck Ex-Vivo Samples.

Ex-vivo samples from patients with head and neck cancer showing the effect of treatment with 0, 1, and10 µM monensin for 48 hours on the expression levels of ATF3, CHOP, and HMG-CoA reductase. The error bars represent SD from the mean of three replicates (n=3).

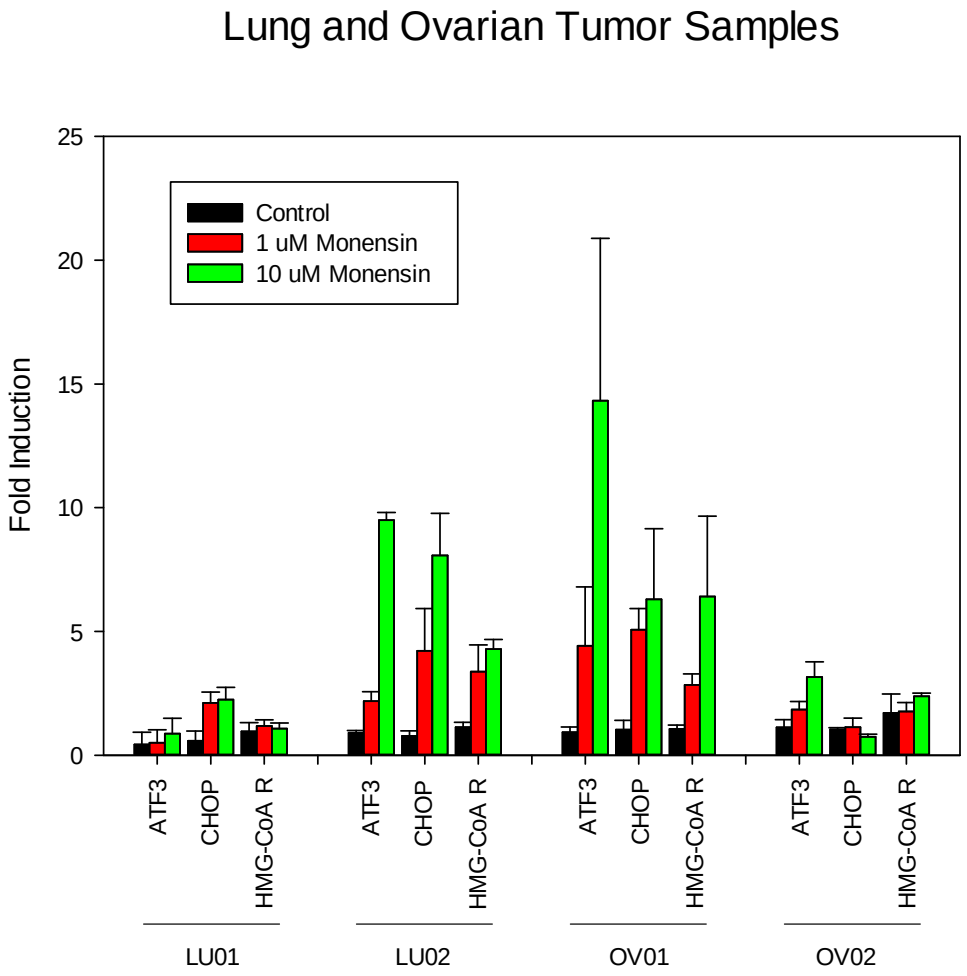

Figure 3.15 RT-PCR Analysis Performed on Ex-Vivo Samples. Ex-vivo samples from patients with lung and ovarian cancer showing the effect of treatment with 0, 1, and10 µM monensin for 48 hours on the expression levels of ATF3, CHOP, and HMG-CoA reductase. The error bars represent SD from the mean of three replicates (n=3).

With 1 µM monensin, ATF3 and CHOP were induced around five fold. Treatment with 10 µM, however, increased ATF3 induction to about 10 times, CHOP and HMG-CoA reductase to around 6 times, while ATF4 stayed around three times. Finally, treatment of OV02 weakly responded to treatment even at 10 µM monensin where the ATF3 induction was around three times higher than control and the rest of the genes were not significantly different from control.

Chapter 4: Discussion

The use of RTKi's in treatment regimens of cancers with a high EGFR over-expression profile, such as NSCLC and HNSCC, has demonstrated a promising although modest improvement in patient outcomes. However, the development and utilization of these agents has contributed to a better understanding of the biology and biochemistry of cancer on the molecular level further revealing particular therapeutic strategies that could be exploited as treatment options. For example, our previous work has identified the mevalonate pathway as an important regulator of EGFR activity and that inhibiting the rate limiting enzyme of this pathway with the statin family of drugs inhibits EGFR activation and can induce synergistic cytotoxicity with gefitinib and erlotinib in HNSCC and NSCLC cells (104). By targeting the prenylation and affecting the cellular localization and function of the Rho family of proteins, ligand-induced dimerization and activation of the EGFR was inhibited as well as inhibition of downstream Akt activation (85). Indeed, a favourable response was shown in patients with NSCLC that were on statins while treated by erlotinib, as shown by Zhao et al. (85); albeit the high statin doses used caused undesirable side effects. In this study, we identified monensin as an enhancer of the EGFR TKi erlotinib and have performed initial studies to discover its mechanism of action in this respect. In summary, monensin

interferes with EGFR cellular trafficking, activates the expression of apoptotic markers and shows synergistic cytotoxicity in combination with erlotinib and activates pathways implicated in lipid and cholesterol synthesis.

4.1 Monensin Exhibits a Cancer-Specific Cytotoxicity

Our results clearly show the cytotoxic effect of monensin in HNSCC derived cell lines, which has also been previously demonstrated in a variety of other cancer derived cell lines including prostate (100), colon (97) and leukemias (98, 99, 101). Furthermore, we also demonstrated that both lovastatin- and erlotinib-induced cytotoxicity was enhanced by the addition of monensin to treatment. Moreover, monensin's cytotoxicity appeared to be cancer-specific as monensin treatment alone or in combination with erlotinib, in the normal fibroblast-derived cell line WI38 did not show a significant cytotoxic response as compared to SCC9 cells. These results are supported by a study by Ketola et al. where they compared malignant versus non-malignant prostate-derived cell lines and showed similar differential sensitivity (100). In addition, Park et al. demonstrated an effect of monensin on cell cycle distribution in a wide panel of cell lines and showed that it has a significant effect on the expression of cyclins and cyclin dependent kinases (CDK). Similarly, our flow cytometry results in SCC9 and SCC25 cells showed decreased G1 and S phases cell distribution with the addition of monensin. Hence, monensin induces apoptosis and reduces cell viability of HNSCC cells.

4.2 Signal and Protein Trafficking is Impaired by Erlotinib, Lovastatin and Monensin

We have shown that monensin enhances the inhibitory effects of erlotinib on ligand-induced phosphorylation of the EGFR. Furthermore, monensin has been used as a reagent to inhibit cellular trafficking and we also demonstrated that this agent can also affect the

localization and trafficking of the EGFR indirectly by following the trafficking of the EGF-Alexa 488 ligand. As expected, erlotinib treatment inhibited the uptake of the ligand as inhibiting autophosphorylation of the receptor prevents docking of adaptor proteins that are responsible for internalizing the receptor from the cell surface. Lovastatin did not significantly inhibit the uptake of the ligand, however, there was an accumulation of the ligand close to the cell surface suggesting that the receptor-ligand complex was internalized but not transported far from the cell surface. Previous studies have shown that by inhibiting prenylation of the Rho proteins, which are involved in cytoskeletal organization, and Rab proteins, which are involved in trafficking (85), lovastatin has the potential to interfere with the trafficking of the EGFR. Furthermore, it is well known that monensin is an inhibitor of trafficking on many levels due to its influence on the ER and golgi bodies, pH of endosomes, and glycosylation (110, 111). In this study we also show that monensin was able to perturb the transport of EGFR from the cell surface. These results are supported by a recent study that showed that accumulation of the EGFR in endosomes induces apoptosis (109). This suggests the combination of these drugs as an effective strategy to target the signalling and trafficking of the EGFR and as a potentially novel therapeutic approach.

4.3 Activation of Apoptotic Pathways and Pathways Implicated in Lipid and Cholesterol Synthesis by Monensin

As previously mentioned, monensin has been used predominantly in poultry and cattle feed as it can increase muscle mass in livestock and only recently it has gained interest as a potentially relevant agent aimed as a therapeutic agent for treatment of human disease. It has been reported by Ketola et al. that monensin has a multitude of effects on cellular functions in a prostate cancer model such as reduction in the expression of androgen receptor, induction of oxidative stress, and activation of cholesterol synthesis pathways and

stress pathways (100). Our data from the RNA-Seq analysis clearly displayed the impact of monensin on those pathways and was confirmed by RT-PCR. Our previous studies have demonstrated the potency of lovastatin, and its combination with RTKi's, to induce apoptosis in a range of cancer-derived cell lines due to its ability to deplete the mevalonate pathway metabolites (78, 84). Moreover, cancer-derived cell lines can also undergo apoptosis when Fatty Acid Synthase (FAS) is inhibited by small molecule inhibitors or siRNA; this was shown to occur due to an up-regulation of DDIT4 which regulates mTOR (112). Although monensin and lovastatin exert a multitude of different effects on cellular metabolism and functions, they both affect pathways important in cholesterol and lipid metabolism. The first evidence in this study that monensin and lovastatin are exerting their effect on a similar pathway is the fact that monensin emerged as an enhancer of both lovastatin and erlotinib in the high throughput Prestwick library screen; although it was not clear whether monensin was mimicking lovastatin or erlotinib. However, when we tested the effect of monensin on the lovastatin-resistant cell line SCC9-R4, which was more sensitive to monensin than the parental cell line, it became evident that monensin is affecting the same pathway albeit by a different mechanism. Based on the data presented, we have constructed a schematic model that shows how these drugs affect cellular functions (Figure 4.1).

Other than the pathways associated with lipid metabolism, monensin also exhibited a significant induction of apoptotic pathways. Treatment of our cell line models, however, showed a disparate response to monensin treatment. The expression profiles of the two cell lines were very different.

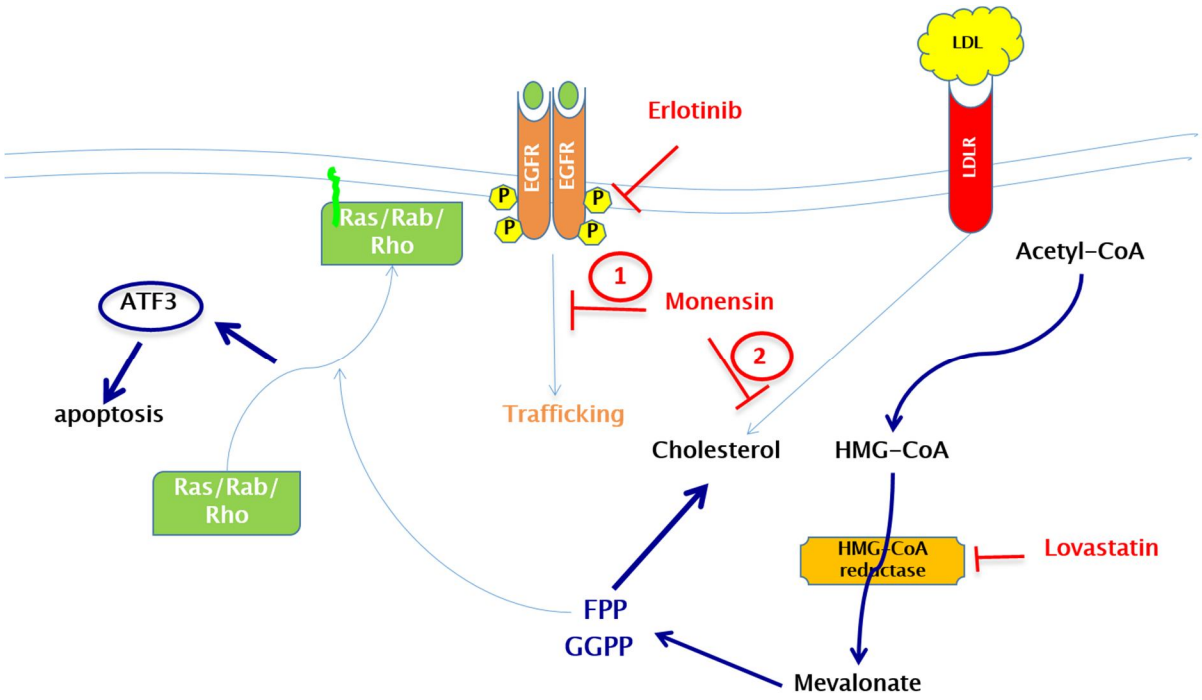

Figure 4.1 Schematic Model. Summary of the effect of treatment based on presented result. Monensin affects the trafficking of EGFR and in combination with erlotinib enhances the inhibition of receptor phosphorylation. Furthermore, in SCC25 cells it inhibits extracellular sources of cholesterol forcing cells to synthesise it locally via the mevalonate pathway, however, both lovastatin and monensin can inhibit the mevalonate pathway leading to depletion of intracellular FPP and GGPP. On the other hand, monensin leads to induction of ATF3 which is an important apoptosis regulator gene.

Of the tested genes, those up-regulated in SCC25 cells were not in SCC9 and those up-regulated in SCC9 cells were not in SCC25. A common gene that was markedly over expressed in both cell lines was the CHOP gene, although to different extents most likely because ATF4 and ATF3 induce CHOP expression (113). It is worth noting that those three genes, the ATF4; ATF3 and CHOP, are a hallmark of the Integrated Stress Response (ISR) which also regulate lovastatin-induced cytotoxicity (114). Up-regulation of CHOP in both cell lines hints towards the idea that in both cell lines monensin is affecting two different pathways that converge on CHOP.

Interestingly, monensin regulates two different pathways that lead to apoptosis as shown by the RT-PCR results in the two SCC cell lines. In the SCC25 cell line, monensin-induced apoptosis appears to be due to perturbation of lipid and cholesterol metabolism, however, in the SCC9 cell line the effect of monensin seems to be regulated by the ISR. As we have cited before, both these pathways have been shown to potentiate the effect of RTKi's. Remarkably, the ex-vivo samples show a response similar to that observed in the cell line models. Some samples showed response by up-regulating genes involved in the stress pathways i.e. ATF3 and CHOP, other samples did not, and some showed induction of both HMG-CoA reductase and stress related genes. Unfortunately, we were limited by the amount of RNA extracted from these ex-vivo samples and could not test the effect of treatment on the other genes involved in lipid and cholesterol metabolism. That being said the results presented in this proposal emphasize the importance of the mentioned pathways in the study of cancer and warrants more research to find out how these pathways are connected and, further, to identify biological markers that will identify patients that would best benefit from such treatment which further advances the use of personalized medicine.

References:

1. **Zhang, Q., N. E. Bhola, V. W. Lui, D. R. Siwak, S. M. Thomas, C. T. Gubish, J. M. Siegfried, G. B. Mills, D. Shin, and J. R. Grandis.** 2007. Antitumor mechanisms of combined gastrin-releasing peptide receptor and epidermal growth factor receptor targeting in head and neck cancer. Mol. Cancer. Ther. **6:**1414-1424. doi: 10.1158/1535-7163.MCT-06-0678.

2. **Mork, J., A. K. Lie, E. Glattre, G. Hallmans, E. Jellum, P. Koskela, B. Moller, E. Pukkala, J. T. Schiller, L. Youngman, M. Lehtinen, and J. Dillner.** 2001. Human papillomavirus infection as a risk factor for squamous-cell carcinoma of the head and neck. N. Engl. J. Med. **344:**1125-1131. doi: 10.1056/NEJM200104123441503.

3. **Khuri, F. R., E. S. Kim, J. J. Lee, R. J. Winn, S. E. Benner, S. M. Lippman, K. K. Fu, J. S. Cooper, E. E. Vokes, R. M. Chamberlain, B. Williams, T. F. Pajak, H. Goepfert, and W. K. Hong.** 2001. The impact of smoking status, disease stage, and index tumor site on second primary tumor incidence and tumor recurrence in the head and neck retinoid chemoprevention trial. Cancer Epidemiol. Biomarkers Prev. **10:**823-829.

4. **Cohen, E. E., M. W. Lingen, and E. E. Vokes.** 2004. The expanding role of systemic therapy in head and neck cancer. J. Clin. Oncol. **22:**1743-1752. doi: 10.1200/JCO.2004.06.147.

5. **Psyrri, A., M. Kwong, S. DiStasio, L. Lekakis, M. Kassar, C. Sasaki, L. D. Wilson, B. G. Haffty, Y. H. Son, D. A. Ross, P. M. Weinberger, G. G. Chung, D. Zelterman, B. A. Burtness, and D. L. Cooper.** 2004. Cisplatin, fluorouracil, and leucovorin induction chemotherapy followed by concurrent cisplatin chemoradiotherapy for organ preservation and cure in patients with advanced head and neck cancer: long-term follow-up. J. Clin. Oncol. **22:**3061-3069. doi: 10.1200/JCO.2004.01.108.

6. **Grandis, J. R., and D. J. Tweardy.** 1993. Elevated levels of transforming growth factor alpha and epidermal growth factor receptor messenger RNA are early markers of carcinogenesis in head and neck cancer. Cancer Res. **53:**3579-3584.

7. **Kalyankrishna, S., and J. R. Grandis.** 2006. Epidermal growth factor receptor biology in head and neck cancer. J. Clin. Oncol. **24:**2666-2672. doi: 10.1200/JCO.2005.04.8306.

8. **Ang, K. K., B. A. Berkey, X. Tu, H. Z. Zhang, R. Katz, E. H. Hammond, K. K. Fu, and L. Milas.** 2002. Impact of epidermal growth factor receptor expression on survival and pattern of relapse in patients with advanced head and neck carcinoma. Cancer Res. **62:**7350-7356.

9. **Salomon, D. S., R. Brandt, F. Ciardiello, and N. Normanno.** 1995. Epidermal growth factor-related peptides and their receptors in human malignancies. Crit. Rev. Oncol. Hematol. **19:**183-232.

10. **Chung, C. H., K. Ely, L. McGavran, M. Varella-Garcia, J. Parker, N. Parker, C. Jarrett, J. Carter, B. A. Murphy, J. Netterville, B. B. Burkey, R. Sinard, A. Cmelak, S. Levy, W. G. Yarbrough, R. J. Slebos, and F. R. Hirsch.** 2006. Increased epidermal growth factor receptor gene copy number is associated with poor prognosis in head and neck squamous cell carcinomas. J. Clin. Oncol. **24:**4170-4176. doi: 10.1200/JCO.2006.07.2587.

11. **Erjala, K., M. Sundvall, T. T. Junttila, N. Zhang, M. Savisalo, P. Mali, J. Kulmala, J. Pulkkinen, R. Grenman, and K. Elenius.** 2006. Signaling via ErbB2 and ErbB3 associates with resistance and epidermal growth factor receptor (EGFR) amplification with sensitivity to EGFR inhibitor gefitinib in head and neck squamous cell carcinoma cells. Clin. Cancer Res. **12:**4103-4111. doi: 10.1158/1078-0432.CCR-05-2404.

12. **Nozawa, H., T. Tadakuma, T. Ono, M. Sato, S. Hiroi, K. Masumoto, and Y. Sato.** 2006. Small interfering RNA targeting epidermal growth factor receptor enhances chemosensitivity to cisplatin, 5-fluorouracil and docetaxel in head and neck squamous cell carcinoma. Cancer. Sci. **97:**1115-1124. doi: 10.1111/j.1349-7006.2006.00287.x.

13. **Seethala, R. R., W. E. Gooding, P. N. Handler, B. Collins, Q. Zhang, J. M. Siegfried, and J. R. Grandis.** 2008. Immunohistochemical analysis of phosphotyrosine signal transducer and activator of transcription 3 and epidermal growth factor receptor autocrine signaling pathways in head and neck cancers and metastatic lymph nodes. Clin. Cancer Res. **14:**1303-1309. doi: 10.1158/1078-0432.CCR-07-1543; 10.1158/1078-0432.CCR-07-1543.

14. **Thomas, S. M., N. E. Bhola, Q. Zhang, S. C. Contrucci, A. L. Wentzel, M. L. Freilino, W. E. Gooding, J. M. Siegfried, D. C. Chan, and J. R. Grandis.** 2006. Cross-talk between G protein-coupled receptor and epidermal growth factor receptor signaling pathways contributes to growth and invasion of head and neck squamous cell carcinoma. Cancer Res. **66:**11831-11839. doi: 10.1158/0008-5472.CAN-06-2876.

15. **Cohen, S., G. Carpenter, and L. King Jr.** 1980. Epidermal growth factor-receptor-protein kinase interactions. Co-purification of receptor and epidermal growth factor-enhanced phosphorylation activity. J. Biol. Chem. **255:**4834-4842.

16. **Davies, R. L., V. A. Grosse, R. Kucherlapati, and M. Bothwell.** 1980. Genetic analysis of epidermal growth factor action: assignment of human epidermal growth factor receptor gene to chromosome 7. Proc. Natl. Acad. Sci. U. S. A. **77:**4188-4192.

17. **Margolis, B., F. Bellot, A. M. Honegger, A. Ullrich, J. Schlessinger, and A. Zilberstein.** 1990. Tyrosine kinase activity is essential for the association of phospholipase C-gamma with the epidermal growth factor receptor. Mol. Cell. Biol. **10:**435-441.

18. **Meisenhelder, J., P. G. Suh, S. G. Rhee, and T. Hunter.** 1989. Phospholipase C-gamma is a substrate for the PDGF and EGF receptor protein-tyrosine kinases in vivo and in vitro. Cell. **57:**1109-1122.

19. **Burgess, A. W., H. -. Cho, C. Eigenbrot, K. M. Ferguson, T. P. J. Garrett, D. J. Leahy, M. A. Lemmon, M. X. Sliwkowski, C. W. Ward, and S. Yokoyama.** 2003. An

open-and-shut case? Recent insights into the activation of EGF/ErbB receptors. Mol. Cell. **12:**541-552.

20. **Yotsumoto, F., H. Yagi, S. O. Suzuki, E. Oki, H. Tsujioka, T. Hachisuga, K. Sonoda, T. Kawarabayashi, E. Mekada, and S. Miyamoto.** 2008. Validation of HB-EGF and amphiregulin as targets for human cancer therapy. Biochem. Biophys. Res. Commun. **365:**555-561. doi: 10.1016/j.bbrc.2007.11.015.

21. **Yarden, Y., and M. X. Sliwkowski.** 2001. Untangling the ErbB signalling network. Nature Reviews Molecular Cell Biology. **2:**127-137.

22. **Moro, L., M. Venturino, C. Bozzo, L. Silengo, F. Altruda, L. Beguinot, G. Tarone, and P. Defilippi.** 1998. Integrins induce activation of EGF receptor: role in MAP kinase induction and adhesion-dependent cell survival. EMBO J. **17:**6622-6632. doi: 10.1093/emboj/17.22.6622.

23. **Zwick, E., H. Daub, N. Aoki, Y. Yamaguchi-Aoki, I. Tinhofer, K. Maly, and A. Ullrich.** 1997. Critical role of calcium- dependent epidermal growth factor receptor transactivation in PC12 cell membrane depolarization and bradykinin signaling. J. Biol. Chem. **272:**24767-24770.

24. **King, C. R., I. Borrello, L. Porter, P. Comoglio, and J. Schlessinger.** 1989. Ligand-independent tyrosine phosphorylation of EGF receptor and the erbB-2/neu proto-oncogene product is induced by hyperosmotic shock. Oncogene. **4:**13-18.

25. **Daub, H., F. U. Weiss, C. Wallasch, and A. Ullrich.** 1996. Role of transactivation of the EGF receptor in signalling by G-protein-coupled receptors. Nature. **379:**557-560. doi: 10.1038/379557a0.

26. **Prenzel, N., E. Zwick, H. Daub, M. Leserer, R. Abraham, C. Wallasch, and A. Ullrich.** 1999. EGF receptor transactivation by G-protein-coupled receptors requires metalloproteinase cleavage of proHB-EGF. Nature. **402:**884-888. doi: 10.1038/47260.

27. **Dawson, J. P., Z. Bu, and M. A. Lemmon.** 2007. Ligand-induced structural transitions in ErbB receptor extracellular domains. Structure. **15:**942-954. doi: 10.1016/j.str.2007.06.013.

28. **Li, S., K. R. Schmitz, P. D. Jeffrey, J. J. W. Wiltzius, P. Kussie, and K. M. Ferguson.** 2005. Structural basis for inhibition of the epidermal growth factor receptor by cetuximab. Cancer Cell. **7:**301-311.

29. **Chang, C. P., C. S. Lazar, B. J. Walsh, M. Komuro, J. F. Collawn, L. A. Kuhn, J. A. Tainer, I. S. Trowbridge, M. G. Farquhar, and M. G. Rosenfeld.** 1993. Ligand-induced internalization of the epidermal growth factor receptor is mediated by multiple endocytic codes analogous to the tyrosine motif found in constitutively internalized receptors. J. Biol. Chem. **268:**19312-19320.

30. **Sorkin, A., C. Waters, K. A. Overholser, and G. Carpenter.** 1991. Multiple autophosphorylation site mutations of the epidermal growth factor receptor. Analysis of kinase activity and endocytosis. J. Biol. Chem. **266:**8355-8362.

31. **Schmidt-Ullrich, R. K., J. N. Contessa, G. Lammering, G. Amorino, and P. S. Lin.** 2003. ERBB receptor tyrosine kinases and cellular radiation responses. Oncogene. **22:**5855-5865. doi: 10.1038/sj.onc.1206698.

32. **Baselga, J., and S. M. Swain.** 2009. Novel anticancer targets: revisiting ERBB2 and discovering ERBB3. Nat. Rev. Cancer. **9:**463-475. doi: 10.1038/nrc2656; 10.1038/nrc2656.

33. **Toulany, M., R. Kehlbach, U. Florczak, A. Sak, S. Wang, J. Chen, M. Lobrich, and H. P. Rodemann.** 2008. Targeting of AKT1 enhances radiation toxicity of human tumor cells by inhibiting DNA-PKcs-dependent DNA double-strand break repair. Mol. Cancer. Ther. **7:**1772-1781. doi: 10.1158/1535-7163.MCT-07-2200; 10.1158/1535-7163.MCT-07-2200.

34. **Golding, S. E., R. N. Morgan, B. R. Adams, A. J. Hawkins, L. F. Povirk, and K. Valerie.** 2009. Pro-survival AKT and ERK signaling from EGFR and mutant EGFRvIII enhances DNA double-strand break repair in human glioma cells. Cancer. Biol. Ther. **8:**730-738.

35. **Kamio, T., K. Shigematsu, H. Sou, K. Kawai, and H. Tsuchiyama.** 1990. Immunohistochemical expression of epidermal growth factor receptors in human adrenocortical carcinoma. Hum. Pathol. **21:**277-282.

36. **Marti, U., S. J. Burwen, A. Wells, M. E. Barker, S. Huling, A. M. Feren, and A. L. Jones.** 1991. Localization of epidermal growth factor receptor in hepatocyte nuclei. Hepatology. **13:**15-20.

37. **Hoshino, M., H. Fukui, Y. Ono, A. Sekikawa, K. Ichikawa, S. Tomita, Y. Imai, J. Imura, H. Hiraishi, and T. Fujimori.** 2007. Nuclear expression of phosphorylated EGFR is associated with poor prognosis of patients with esophageal squamous cell carcinoma. Pathobiology. **74:**15-21. doi: 10.1159/000101047.

38. **Li, C., M. Iida, E. F. Dunn, A. J. Ghia, and D. L. Wheeler.** 2009. Nuclear EGFR contributes to acquired resistance to cetuximab. Oncogene. **28:**3801-3813. doi: 10.1038/onc.2009.234; 10.1038/onc.2009.234.

39. **Li, C., M. Iida, E. F. Dunn, and D. L. Wheeler.** 2010. Dasatinib blocks cetuximab- and radiation-induced nuclear translocation of the epidermal growth factor receptor in head and neck squamous cell carcinoma. Radiother. Oncol. **97:**330-337. doi: 10.1016/j.radonc.2010.06.010; 10.1016/j.radonc.2010.06.010.

40. **Matar, P., F. Rojo, R. Cassia, G. Moreno-Bueno, S. Di Cosimo, J. Tabernero, M. Guzman, S. Rodriguez, J. Arribas, J. Palacios, and J. Baselga.** 2004. Combined epidermal growth factor receptor targeting with the tyrosine kinase inhibitor gefitinib (ZD1839) and the monoclonal antibody cetuximab (IMC-C225): superiority over single-

agent receptor targeting. Clin. Cancer Res. **10:**6487-6501. doi: 10.1158/1078-0432.CCR-04-0870.

41. **Zhang, Q., S. M. Thomas, S. Xi, T. E. Smithgall, J. M. Siegfried, J. Kamens, W. E. Gooding, and J. R. Grandis.** 2004. SRC family kinases mediate epidermal growth factor receptor ligand cleavage, proliferation, and invasion of head and neck cancer cells. Cancer Res. **64:**6166-6173. doi: 10.1158/0008-5472.CAN-04-0504.

42. **Yoshida, T., I. Okamoto, T. Iwasa, M. Fukuoka, and K. Nakagawa.** 2008. The anti-EGFR monoclonal antibody blocks cisplatin-induced activation of EGFR signaling mediated by HB-EGF. FEBS Lett. **582:**4125-4130. doi: 10.1016/j.febslet.2008.11.010; 10.1016/j.febslet.2008.11.010.

43. **Fan, Z., Y. Lu, X. Wu, and J. Mendelsohn.** 1994. Antibody-induced epidermal growth factor receptor dimerization mediates inhibition of autocrine proliferation of A431 squamous carcinoma cells. J. Biol. Chem. **269:**27595-27602.

44. **Mandic, R., C. J. Rodgarkia-Dara, L. Zhu, B. J. Folz, M. Bette, E. Weihe, A. Neubauer, and J. A. Werner.** 2006. Treatment of HNSCC cell lines with the EGFR-specific inhibitor cetuximab (ErbituxÂ®) results in paradox phosphorylation of tyrosine 1173 in the receptor. FEBS Lett. **580:**4793-4800.

45. **Almand, B., J. R. Resser, B. Lindman, S. Nadaf, J. I. Clark, E. D. Kwon, D. P. Carbone, and D. I. Gabrilovich.** 2000. Clinical significance of defective dendritic cell differentiation in cancer. Clin. Cancer Res. **6:**1755-1766.

46. **Mickel, R. A., D. J. Kessler, J. M. Taylor, and A. Lichtenstein.** 1988. Natural killer cell cytotoxicity in the peripheral blood, cervical lymph nodes, and tumor of head and neck cancer patients. Cancer Res. **48:**5017-5022.

47. **Bonner, J. A., P. M. Harari, J. Giralt, N. Azarnia, D. M. Shin, R. B. Cohen, C. U. Jones, R. Sur, D. Raben, J. Jassem, R. Ove, M. S. Kies, J. Baselga, H. Youssoufian, N. Amellal, E. K. Rowinsky, and K. K. Ang.** 2006. Radiotherapy plus cetuximab for squamous-cell carcinoma of the head and neck. N. Engl. J. Med. **354:**567-578. doi: 10.1056/NEJMoa053422.

48. **Gee, J. E., I. Robbins, A. C. van der Laan, J. H. van Boom, C. Colombier, M. Leng, A. M. Raible, J. S. Nelson, and B. Lebleu.** 1998. Assessment of high-affinity hybridization, RNase H cleavage, and covalent linkage in translation arrest by antisense oligonucleotides. Antisense Nucleic Acid Drug Dev. **8:**103-111.

49. **Ketting, R. F., S. E. Fischer, E. Bernstein, T. Sijen, G. J. Hannon, and R. H. Plasterk.** 2001. Dicer functions in RNA interference and in synthesis of small RNA involved in developmental timing in C. elegans. Genes Dev. **15:**2654-2659. doi: 10.1101/gad.927801.

50. **Elbashir, S. M., W. Lendeckel, and T. Tuschl.** 2001. RNA interference is mediated by 21- and 22-nucleotide RNAs. Genes Dev. **15:**188-200.

51. **Schwarz, D. S., G. Hutvagner, T. Du, Z. Xu, N. Aronin, and P. D. Zamore.** 2003. Asymmetry in the assembly of the RNAi enzyme complex. Cell. **115:**199-208.

52. **Song, J. J., S. K. Smith, G. J. Hannon, and L. Joshua-Tor.** 2004. Crystal structure of Argonaute and its implications for RISC slicer activity. Science. **305:**1434-1437. doi: 10.1126/science.1102514.

53. **He, Y., Q. Zeng, S. D. Drenning, M. F. Melhem, D. J. Tweardy, L. Huang, and J. R. Grandis.** 1998. Inhibition of human squamous cell carcinoma growth in vivo by epidermal growth factor receptor antisense RNA transcribed from the U6 promoter. J. Natl. Cancer Inst. **90:**1080-1087.

54. **Bachran, C., M. Sutherland, D. Bachran, and H. Fuchs.** 2007. Quantification of diphtheria toxin mediated ADP-ribosylation in a solid-phase assay. Clin. Chem. **53:**1676-1683. doi: 10.1373/clinchem.2007.085365.

55. **Phillips, P. C., C. Levow, M. Catterall, O. M. Colvin, I. Pastan, and H. Brem.** 1994. Transforming growth factor-alpha-Pseudomonas exotoxin fusion protein (TGF-alpha-PE38) treatment of subcutaneous and intracranial human glioma and medulloblastoma xenografts in athymic mice. Cancer Res. **54:**1008-1015.

56. **Thomas, S. M., Q. Zeng, M. W. Epperly, W. E. Gooding, I. Pastan, Q. C. Wang, J. Greenberger, and J. R. Grandis.** 2004. Abrogation of head and neck squamous cell carcinoma growth by epidermal growth factor receptor ligand fused to pseudomonas exotoxin transforming growth factor alpha-PE38. Clin. Cancer Res. **10:**7079-7087. doi: 10.1158/1078-0432.CCR-04-0587.

57. **Stamos, J., M. X. Sliwkowski, and C. Eigenbrot.** 2002. Structure of the epidermal growth factor receptor kinase domain alone and in complex with a 4-anilinoquinazoline inhibitor. J. Biol. Chem. **277:**46265-46272. doi: 10.1074/jbc.M207135200.

58. **Baselga, J., D. Rischin, M. Ranson, H. Calvert, E. Raymond, D. G. Kieback, S. B. Kaye, L. Gianni, A. Harris, T. Bjork, S. D. Averbuch, A. Feyereislova, H. Swaisland, F. Rojo, and J. Albanell.** 2002. Phase I safety, pharmacokinetic, and pharmacodynamic trial of ZD1839, a selective oral epidermal growth factor receptor tyrosine kinase inhibitor, in patients with five selected solid tumor types. Journal of Clinical Oncology. **20:**4292-4302.

59. **Hidalgo, M., L. L. Siu, J. Nemunaitis, J. Rizzo, L. A. Hammond, C. Takimoto, S. G. Eckhardt, A. Tolcher, C. D. Britten, L. Denis, K. Ferrante, D. D. Von Hoff, S. Silberman, and E. K. Rowinsky.** 2001. Phase I and pharmacologic study of OSI-774, an epidermal growth factor receptor tyrosine kinase inhibitor, in patients with advanced solid malignancies. Journal of Clinical Oncology. **19:**3267-3279.

60. **Fukuoka, M., S. Yano, G. Giaccone, T. Tamura, K. Nakagawa, J. -. Douillard, Y. Nishiwaki, J. Vansteenkiste, S. Kudoh, D. Rischin, R. Eek, T. Horai, K. Noda, I. Takata, E. Smit, S. Averbuch, A. Macleod, A. Feyereislova, R. -. Dong, and J. Baselga.** 2003. Multi-institutional randomized phase II trial of gefitinib for previously treated patients with advanced non-small-cell lung cancer. Journal of Clinical Oncology. **21:**2237-2246.

61. **Kris, M. G., R. B. Natale, R. S. Herbst, T. J. Lynch Jr., D. Prager, C. P. Belani, J. H. Schiller, K. Kelly, H. Spiridonidis, A. Sandler, K. S. Albain, D. Cella, M. K. Wolf, S. D. Averbuch, J. J. Ochs, and A. C. Kay.** 2003. Efficacy of Gefitinib, an Inhibitor of the Epidermal Growth Factor Receptor Tyrosine Kinase, in Symptomatic Patients with Non-Small Cell Lung Cancer: A Randomized Trial. J. Am. Med. Assoc. **290:**2149-2158.

62. **Giaccone, G., R. S. Herbst, C. Manegold, G. Scagliotti, R. Rosell, V. Miller, R. B. Natale, J. H. Schiller, J. Von Pawel, A. Pluzanska, U. Gatzemeier, J. Grous, J. S. Ochs, S. D. Averbuch, M. K. Wolf, P. Rennie, A. Fandi, and D. H. Johnson.** 2004. Gefitinib in combination with gemcitabine and cisplatin in advanced non-small-cell lung cancer: A phase III trial - INTACT 1. Journal of Clinical Oncology. **22:**777-784.

63. **Herbst, R. S., G. Giaccone, J. H. Schiller, R. B. Natale, V. Miller, C. Manegold, G. Scagliotti, R. Rosell, I. Oliff, J. A. Reeves, M. K. Wolf, A. D. Krebs, S. D. Averbuch, J. S. Ochs, J. Grous, A. Fandi, and D. H. Johnson.** 2004. Gefitinib in combination with paclitaxel and carboplatin in advanced non-small-cell lung cancer: A phase III trial - INTACT 2. Journal of Clinical Oncology. **22:**785-794.

64. **Shepherd, F. A., J. R. Pereira, T. Ciuleanu, H. T. Eng, V. Hirsh, S. Thongprasert, D. Campos, S. Maoleekoonpiroj, M. Smylie, R. Martins, M. Van Kooten, M. Dediu, B. Findlay, D. Tu, D. Johnston, A. Bezjak, G. Clark, P. SantabÃ¡rbara, and L. Seymour.** 2005. Erlotinib in previously treated non-small-cell lung cancer. N. Engl. J. Med. **353:**123-132.

65. **Paez, J. G., P. A. JÃ¤nne, J. C. Lee, S. Tracy, H. Greulich, S. Gabriel, P. Herman, F. J. Kaye, N. Lindeman, T. J. Boggon, K. Naoki, H. Sasaki, Y. Fujii, M. J. Eck, W. R. Sellers, B. E. Johnson, and M. Meyerson.** 2004. EGFR mutations in lung, cancer: Correlation with clinical response to gefitinib therapy. Science. **304:**1497-1500.

66. **Lynch, T. J., D. W. Bell, R. Sordella, S. Gurubhagavatula, R. A. Okimoto, B. W. Brannigan, P. L. Harris, S. M. Haserlat, J. G. Supko, F. G. Haluska, D. N. Louis, D. C. Christiani, J. Settleman, and D. A. Haber.** 2004. Activating Mutations in the Epidermal Growth Factor Receptor Underlying Responsiveness of Non-Small-Cell Lung Cancer to Gefitinib. N. Engl. J. Med. **350:**2129-2139.

67. **Wheeler, D. L., S. Huang, T. J. Kruser, M. M. Nechrebecki, E. A. Armstrong, S. Benavente, V. Gondi, K. -. Hsu, and P. M. Harari.** 2008. Mechanisms of acquired resistance to cetuximab: Role of HER (ErbB) family members. Oncogene. **27:**3944-3956.

68. **Balak, M. N., Y. Gong, G. J. Riely, R. Somwar, A. R. Li, M. F. Zakowski, A. Chiang, G. Yang, O. Ouerfelli, M. G. Kris, M. Ladanyi, V. A. Miller, and W. Pao.** 2006. Novel D761Y and common secondary T790M mutations in epidermal growth factor receptor-mutant lung adenocarcinomas with acquired resistance to kinase inhibitors. Clinical Cancer Research. **12:**6494-6501.

69. **Stabile, L. P., G. He, V. W. Lui, C. Henry, C. T. Gubish, S. Joyce, K. M. Quesnelle, J. M. Siegfried, and J. R. Grandis.** 2013. c-Src activation mediates erlotinib resistance in

head and neck cancer by stimulating c-Met. Clin. Cancer Res. **19:**380-392. doi: 10.1158/1078-0432.CCR-12-1555; 10.1158/1078-0432.CCR-12-1555.

70. **Alberts, A. W., J. Chen, G. Kuron, V. Hunt, J. Huff, C. Hoffman, J. Rothrock, M. Lopez, H. Joshua, E. Harris, A. Patchett, R. Monaghan, S. Currie, E. Stapley, G. Albers-Schonberg, O. Hensens, J. Hirshfield, K. Hoogsteen, J. Liesch, and J. Springer.** 1980. Mevinolin: a highly potent competitive inhibitor of hydroxymethylglutaryl-coenzyme A reductase and a cholesterol-lowering agent. Proc. Natl. Acad. Sci. U. S. A. **77:**3957-3961.

71. **Goldstein, J. L., and M. S. Brown.** 1990. Regulation of the mevalonate pathway. Nature. **343:**425-430. doi: 10.1038/343425a0.

72. **Sebti, S., and A. D. Hamilton.** 1997. Inhibitors of prenyl transferases. Curr. Opin. Oncol. **9:**557-561.

73. **Hancock, J. F., A. I. Magee, J. E. Childs, and C. J. Marshall.** 1989. All ras proteins are polyisoprenylated but only some are palmitoylated. Cell. **57:**1167-1177.

74. **Reiss, Y., J. L. Goldstein, M. C. Seabra, P. J. Casey, and M. S. Brown.** 1990. Inhibition of purified p21ras farnesyl:protein transferase by Cys-AAX tetrapeptides. Cell. **62:**81-88.

75. **Pruitt, K., and C. J. Der.** 2001. Ras and Rho regulation of the cell cycle and oncogenesis. Cancer Lett. **171:**1-10.

76. **Thibault, A., D. Samid, A. C. Tompkins, W. D. Figg, M. R. Cooper, R. J. Hohl, J. Trepel, B. Liang, N. Patronas, D. J. Venzon, E. Reed, and C. E. Myers.** 1996. Phase I study of lovastatin, an inhibitor of the mevalonate pathway, in patients with cancer. Clin. Cancer Res. **2:**483-491.

77. **Larner, J., J. Jane, E. Laws, R. Packer, C. Myers, and M. Shaffrey.** 1998. A phase I-II trial of lovastatin for anaplastic astrocytoma and glioblastoma multiforme. Am. J. Clin. Oncol. **21:**579-583.

78. **Dimitroulakos, J., L. Y. Ye, M. Benzaquen, M. J. Moore, S. Kamel-Reid, M. H. Freedman, H. Yeger, and L. Z. Penn.** 2001. Differential sensitivity of various pediatric cancers and squamous cell carcinomas to lovastatin-induced apoptosis: therapeutic implications. Clin. Cancer Res. **7:**158-167.

79. **Dimitroulakos, J., D. Nohynek, K. L. Backway, D. W. Hedley, H. Yeger, M. H. Freedman, M. D. Minden, and L. Z. Penn.** 1999. Increased sensitivity of acute myeloid leukemias to lovastatin-induced apoptosis: A potential therapeutic approach. Blood. **93:**1308-1318.

80. **Knox, J. J., L. L. Siu, E. Chen, J. Dimitroulakos, S. Kamel-Reid, M. J. Moore, S. Chin, J. Irish, S. LaFramboise, and A. M. Oza.** 2005. A Phase I trial of prolonged administration of lovastatin in patients with recurrent or metastatic squamous cell carcinoma

of the head and neck or of the cervix. Eur. J. Cancer. **41:**523-530. doi: 10.1016/j.ejca.2004.12.013.

81. **Gschwind, A., O. M. Fischer, and A. Ullrich.** 2004. The discovery of receptor tyrosine kinases: Targets for cancer therapy. Nature Reviews Cancer. **4:**361-370.

82. **Hallberg, B., S. I. Rayter, and J. Downward.** 1994. Interaction of Ras and Raf in intact mammalian cells upon extracellular stimulation. J. Biol. Chem. **269:**3913-3916.

83. **Gibbs, J. B., A. Oliff, and N. E. Kohl.** 1994. Farnesyltransferase inhibitors: Ras research yields a potential cancer therapeutic. Cell. **77:**175-178.

84. **Mantha, A. J., J. E. Hanson, G. Goss, A. E. Lagarde, I. A. Lorimer, and J. Dimitroulakos.** 2005. Targeting the mevalonate pathway inhibits the function of the epidermal growth factor receptor. Clin. Cancer Res. **11:**2398-2407. doi: 10.1158/1078-0432.CCR-04-1951.

85. **Zhao, T. T., B. G. Le Francois, G. Goss, K. Ding, P. A. Bradbury, and J. Dimitroulakos.** 2010. Lovastatin inhibits EGFR dimerization and AKT activation in squamous cell carcinoma cells: potential regulation by targeting rho proteins. Oncogene. **29:**4682-4692. doi: 10.1038/onc.2010.219; 10.1038/onc.2010.219.

86. **Campbell, W. C.** 2008. History of the discovery of sulfaquinoxaline as a coccidiostat. J. Parasitol. **94:**934-945.

87. **Agtarap, A., J. W. Chamberlin, M. Pinkerton, and L. Steinrauf.** 1967. The structure of monensic acid, A new biologically active compound [27]. J. Am. Chem. Soc. **89:**5737-5739.

88. **Van Vleet, J. F., H. E. Amstutz, W. E. Weirich, A. H. Rebar, and V. J. Ferrans.** 1983. Clinical, clinicopathologic, and pathologic alterations in acute monensin toxicosis in cattle. Am. J. Vet. Res. **44:**2133-2144.

89. **Pressman, B. C.** 1976. Biological applications of ionophores. Annu. Rev. Biochem. **Vol. 45:**501-530.

90. **Pressman, B. C.** 1968. Ionophorous antibiotics as models for biological transport. Fed. Proc. **27:**1283-1288.

91. **Pressman, B. C., and M. Fahim.** 1982. Pharmacology and toxicology of the monovalent carboxylic ionophores. Annu. Rev. Pharmacol. Toxicol. **22:**465-490.

92. **Estrada-O, S.** 1968. Antibiotics as tools for metabolic studies. X1. Specific inhibition of ion transport in mitochondria by the monensins. Antimicrob. Agents Chemother. **1967:**279-288.

93. **Ryley, J. F., and M. J. Betts.** 1973. Chemotherapy of Chicken Coccidiosis. Adv. Pharmacol. **11:**221-293.

94. **Smith II, C. K., and R. B. Galloway.** 1983. Influence of monensin on cation influx and glycolysis of Eimeria tenella sporozoites in vitro. J. Parasitol. **69:**666-670.

95. **Del Cacho, E., M. Gallego, C. SÃ¡nchez-Acedo, and H. S. Lillehoj.** 2007. Expression of flotillin-1 on Eimeria tenella sporozoites and its role in host cell invasion. J. Parasitol. **93:**328-332.

96. **Park, W. H., C. W. Jung, J. O. Park, K. Kim, W. S. Kim, Y. H. Im, M. H. Lee, W. K. Kang, and K. Park.** 2003. Monensin inhibits the growth of renal cell carcinoma cells via cell cycle arrest or apoptosis. Int. J. Oncol. **22:**855-860.

97. **Park, W. H., E. S. Kim, C. W. Jung, B. K. Kim, and Y. Y. Lee.** 2003. Monensin-mediated growth inhibition of SNU-C1 colon cancer cells via cell cycle arrest and apoptosis. Int. J. Oncol. **22:**377-382.

98. **Park, W. H., E. S. Kim, B. K. Kim, and Y. Y. Lee.** 2003. Monensin-mediated growth inhibition in NCI-H929 myeloma cells via cell cycle arrest and apoptosis. Int. J. Oncol. **23:**197-204.

99. **Park, W. H., J. G. Seol, E. S. Kim, W. K. Kang, Y. H. Im, C. W. Jung, B. K. Kim, and Y. Y. Lee.** 2002. Monensin-mediated growth inhibition in human lymphoma cells through cell cycle arrest and apoptosis. Br. J. Haematol. **119:**400-407.

100. **Ketola, K., P. Vainio, V. Fey, O. Kallioniemi, and K. Iljin.** 2010. Monensin is a potent inducer of oxidative stress and inhibitor of androgen signaling leading to apoptosis in prostate cancer cells. Mol. Cancer. Ther. **9:**3175-3185. doi: 10.1158/1535-7163.MCT-10-0368; 10.1158/1535-7163.MCT-10-0368.

101. **Park, W. H., M. S. Lee, K. Park, E. S. Kim, B. K. Kim, and Y. Y. Lee.** 2002. Monensin-mediated growth inhibition in acute myelogenous leukemia cells via cell cycle arrest and apoptosis. Int. J. Cancer. **101:**235-242. doi: 10.1002/ijc.10592.

102. **Pinthus, J. H., I. Bryskin, J. Trachtenberg, J. -. Lu, G. Singh, E. Fridman, and B. C. Wilson.** 2007. Androgen induces adaptation to oxidative stress in prostate cancer: Implications for treatment with radiation therapy. Neoplasia. **9:**68-80.

103. **Huczynski, A., J. Stefanska, P. Przybylski, B. Brzezinski, and F. Bartl.** 2008. Synthesis and antimicrobial properties of monensin A esters. Bioorg. Med. Chem. Lett. **18:**2585-2589. doi: 10.1016/j.bmcl.2008.03.038; 10.1016/j.bmcl.2008.03.038.

104. **Dimitroulakos, J., I. A. Lorimer, and G. Goss.** 2006. Strategies to enhance epidermal growth factor inhibition: targeting the mevalonate pathway. Clin. Cancer Res. **12:**4426s-4431s. doi: 10.1158/1078-0432.CCR-06-0089.

105. **Chomczynski, P., and K. Mackey.** 1995. Short technical reports. Modification of the TRI reagent procedure for isolation of RNA from polysaccharide- and proteoglycan-rich sources. BioTechniques. **19:**942-945.

106. **Wang, Q., G. Villeneuve, and Z. Wang.** 2005. Control of epidermal growth factor receptor endocytosis by receptor dimerization, rather than receptor kinase activation. EMBO Rep. **6:**942-948. doi: 10.1038/sj.embor.7400491.

107. **Chou, T. -., and P. Talalay.** 1984. Quantitative analysis of dose-effect relationships: the combined effects of multiple drugs or enzyme inhibitors. Adv. Enzyme Regul. **22:**27-55.

108. **Gladhaug, I. P., and T. Christoffersen.** 1988. Rapid constitutive internalization and externalization of epidermal growth factor receptors in isolated rat hepatocytes. Monensin inhibits receptor externalization and reduces the capacity for continued endocytosis of epidermal growth factor. J. Biol. Chem. **263:**12199-12203.

109. **Rush, J. S., L. M. Quinalty, L. Engelman, D. M. Sherry, and B. P. Ceresa.** 2012. Endosomal accumulation of the activated epidermal growth factor receptor (EGFR) induces apoptosis. J. Biol. Chem. **287:**712-722. doi: 10.1074/jbc.M111.294470; 10.1074/jbc.M111.294470.

110. **Mollenhauer, H. H., D. J. Morre, and L. D. Rowe.** 1990. Alteration of intracellular traffic by monensin; mechanism, specificity and relationship to toxicity. Biochimica Et Biophysica Acta - Reviews on Biomembranes. **1031:**225-246.

111. **Tartakoff, A. M.** 1983. Perturbation of vesicular traffic with the carboxylic ionophore monensin. Cell. **32:**1026-1028.

112. **Knowles, L. M., C. Yang, A. Osterman, and J. W. Smith.** 2008. Inhibition of fatty-acid synthase induces caspase-8-mediated tumor cell apoptosis by up-regulating DDIT4. J. Biol. Chem. **283:**31378-31384. doi: 10.1074/jbc.M803384200; 10.1074/jbc.M803384200.

113. **Jiang, H. Y., S. A. Wek, B. C. McGrath, D. Lu, T. Hai, H. P. Harding, X. Wang, D. Ron, D. R. Cavener, and R. C. Wek.** 2004. Activating transcription factor 3 is integral to the eukaryotic initiation factor 2 kinase stress response. Mol. Cell. Biol. **24:**1365-1377.

114. **Niknejad, N., M. Morley, and J. Dimitroulakos.** 2007. Activation of the integrated stress response regulates lovastatin-induced apoptosis. J. Biol. Chem. **282:**29748-29756. doi: 10.1074/jbc.M705859200.

Contributions of Collaborators

- Initial Prestwick library screen was performed by Stefanie Reid.
- MTT assays of the SCC25 and SCC9 cell lines were performed by a University of Ottawa co-op student in our lab, Janet Barber.
- RT-PCR on the ex-vivo patient samples were performed with the help of our laboratory technician Ivan Gorn-Hunderman.

Appendix I: Ethics approval

Research Ethics Board approval for working with human head and neck, lung and ovarian cancer tumours: OREB # 2012 0559-01H

Curriculum Vitae

Khalil Dayekh

Work Experience

February 2010 – July 2011: Sears parts and service Ottawa, ON.
Sales and support associate:

- Operated cash register.
- Maintained inventory and stock.
- Booked customers' appliances for servicing, and phone customers when their appliances were fixed to pick them up.
- Helped customers find specific parts they required for their appliances.
- Ordered parts for customers if not in stock, and phoned them when the parts were in store for pick up.
- Supplied technicians with parts they needed to fix customers' appliances at home or at the repair shop.
- Handled received shipments, matched parts coming from central warehouse with manifest; shipped surplus parts to central warehouse.

January 2010 – February 2010 WIS international Ottawa, ON.
Inventory Clerk:

- Counted client inventory with high accuracy and efficiency.
- Recorded counts and amounts on inventory tags.
- Proficient in using the WISard inventory instrument.
- Performed financial and basic SKU counts.

June 2008 – September 2008 Natural Resources Canada Ottawa, ON.
Senior Procurement Clerk:

- Provided financial services to clients in accordance with the financial administration act (FAA) and other legislation and agreements.
- Reviewed requisition orders for accuracy.
- Verified stock availability from current inventories.
- Obtained price quotations from catalogues and suppliers.
- Forwarded invoices to appropriate accounts.
- Processed purchases.
- Resolved delivery and other problems with suppliers.
- Prepared and maintained purchasing files, reports and records.
- Performed routine clerical duties.
- Delivered services within established guidelines related to quantity, quality and timeliness as outlined in respective service agreements with clients.
- Worked with GUFI software to generate contracts.
- Generated and processed around 80 contracts including purchase orders, call-ups against standing offers and task authorizations.
- Handled contracts with values up to 45,000 dollars.

Education

January 2011 – current University of Ottawa Ottawa, ON.

Currently attending University of Ottawa for a Master's degree in biochemistry with specialization in human and molecular genetics, and performing research in the Ottawa Hospital Research Institute at the cancer center. Co-authored a paper in the scientific journal Plos One in Septembe 2012, and currently collaborating in three more studies for future publications.

September 2005 – April 2010 University of Ottawa Ottawa, ON.

- Obtained a Bachelor's degree in Honors and specialization in Biochemistry.
- Able to perform basic scientific experiments using current methods.
- Have experience in preparation of written reports related to scientific data.

Volunteering Expreince

- Supervised a high school student in the laboratory for her cooperative education program.
- Member of the Lets Talk Science community for helping students, from kindergarten to highschool, learn more about science.
- Took part in the "Math Help Center" to help students with their mathematics skills and problems at the Adult High School.
- Member of Al-Ansar youth club.

Awards

- Placed on the "Dean's Honor List" for the academic year 2009-2010.
- Awarded the "Student of the Month for Science" for November 2004.
- Awarded the "Alumni Award for Scholastic Merit University" June 2004.
- Awarded the Cooperative Education Certificate of Appreciation for active participation in and support of the cooperative education program.